Hydrol. Earth Syst. Sci., 29, 5405–5427, 2025 https://doi.org/10.5194/hess-29-5405-2025 © Author(s) 2025. This work is distributed under the Creative Commons Attribution 4.0 License.





# Can we reliably estimate precipitation with high resolution during disastrously large floods?

 ${\bf Jan\ Szturc^1, Anna\ Jurczyk^1, Katarzyna\ Ośródka^1, Agnieszka\ Kurcz^1, Magdalena\ Szaton^1, Mariusz\ Figurski^2, and\ Robert\ Pyrc^3}$ 

<sup>1</sup>Institute of Meteorology and Water Management – National Research Institute,

Centre of the Weather Forecasting Service, Warszawa, Poland

ricusurement and Observation retwork Centre, warszawa, rotand

Correspondence: Jan Szturc (jan.szturc@imgw.pl) and Anna Jurczyk (anna.jurczyk@imgw.pl)

Received: 18 April 2025 – Discussion started: 19 May 2025

Revised: 1 August 2025 - Accepted: 26 August 2025 - Published: 21 October 2025

Abstract. A huge and dangerous flood occurred in September 2024 in the upper and middle Odra River basin, including mountainous areas, in south-western Poland. The event provided an opportunity to investigate the feasibility of a reliable estimation of a high-resolution precipitation field, which is crucial for effective flood protection. Data from different measurement techniques were analysed: rain gauges, weather radars, satellites, and commercial microwave links (CMLs) and multi-source estimation. Apart from real-time and near-real-time data, later available reanalyses based on satellite information (IMERG, PDIR-Now) and numerical mesoscale model simulations (ERA5, WRF) were also examined. Reference data used to verify the reliability of the different techniques for the measurement and estimation of precipitation included observations from manual rain gauges and multi-source estimates from the RainGRS system developed at the Institute of Meteorology and Water Management - National Research Institute (IMGW) for daily and hourly accumulations, respectively. Statistical analyses and visual comparisons were carried out. Among the data available in real time, the best results were found for rain gauge measurements, radar data adjusted to rain gauges, and RainGRS estimates. Fairly good reliability was achieved by non-conventional CML-based measurements. In terms of offline reanalyses, mesoscale model simulations also demonstrated reasonably good agreement with reference precipitation, while poorer results were obtained by all satellite-based estimates except IMERG.

#### 1 Introduction

#### 1.1 Motivation

Precipitation is one of the most important meteorological parameters. In the case of extreme weather events, the precise estimation of the precipitation field with high spatial resolution, preferably carried out in real time, is of crucial importance for effective flood protection (Sokol et al., 2021; Velásquez et al., 2025), especially in mountainous regions. The accurate determination of precipitation amounts is also important for subsequent studies and expert opinions. In this context, the following question arises: are we able to measure precipitation with sufficient reliability to carry out these tasks? The ability to estimate precipitation either in real time or in near real time (i.e. with a delay of up to several minutes, half an hour at most) is crucial, but data available afterwards for detailed analysis are also valuable.

Knowledge of the high-resolution spatial distribution of precipitation in real time provides the basis for generating forecasts with high resolution in time and space. Based on an extrapolation approach, nowcasting models (very-short-range forecasting) generate such forecasts with very high precision but with a relatively short lead time (Bojinski et al., 2023). This is particularly important when monitoring and forecasting severe convective phenomena (Fischer et al., 2025) for effective flood protection.

The main problem in analysing the accuracy of such forecasts is the lack of a reliable reference with a sufficiently

<sup>&</sup>lt;sup>2</sup>Gdansk University of Technology, Faculty of Civil and Environmental Engineering, Department of Geodesy, Gdańsk, Poland

<sup>&</sup>lt;sup>3</sup>Institute of Meteorology and Water Management – National Research Institute, Hydrological and Meteorological Measurement and Observation Network Centre, Warszawa, Poland

high spatial and temporal resolution. Such a reference could be the most reliable measurements or reanalyses available offline. Manual rain gauge measurements, which are most often available in the form of daily accumulations, are usually used as a reference for other measurements and estimates (e.g. Hoffmann et al., 2016). However, rain gauges only provide point measurements, making spatial representation of precipitation highly dependent on network density. In the case of a sparse network and highly spatially variable precipitation, its accurate reconstruction becomes nearly impossible. Therefore, it is necessary to carry out various comparative analyses using all available measurement and estimation techniques to select optimal solutions (Hohmann et al., 2021; Loritz et al., 2021).

#### 1.2 State of the art

# 1.2.1 High-resolution measurements of precipitation during extreme weather events

In the operational practice of the National Meteorological and Hydrological Services (NMHSs), the most commonly used rainfall measurement techniques are in situ measurements made with various types of rain gauges, weather radar observations, and satellite-derived estimates. These measurements vary in spatial resolution, technical limitations, and sensitivity to various disturbing factors; consequently, measurement errors have a completely different structure.

Rain gauges measure rainfall point-wise, i.e. only at their locations, and their reliability is affected by various factors related to meteorological conditions as well as to the failure rate and precision of the measurement, which is dependent on their design. This technique is considered the most accurate of those currently in use but only in respect of the measurement location. Primarily, in the case of sparse rain gauge networks, point measurements do not provide reliable precipitation fields with a sufficiently high spatial resolution. One way to enhance the coverage of a given area with rain gauge measurements is to add data from personal weather stations (Garcia-Marti et al., 2023; Overeem et al., 2024).

Weather radars measure the spatial distribution of the precipitation field with a very high resolution of the order of 1 km, which depends on the distance from the radar site. However, radar data are sensitive to a wide variety of disturbances, such as the interaction of the radar beam with the terrain and objects on it, varying signal propagation conditions, interference with signals from other devices emitting microwave signals (e.g. radio local area network (RLAN) transmitters), and many others. As a result, sophisticated quality control algorithms are necessary, although they are not completely effective (Méri et al., 2021; Ośródka and Szturc, 2022).

Operationally, the least reliable methods are those based on satellite imagery in the various spectral channels: microwave, which is the most technically challenging, as well as visible (VIS) and infrared (IR). Although satellite data are generally widely available, their reliability, except for microwave data, are relatively low, making them less commonly used in operational applications than rain gauge and radar data. In addition, their accuracy depends strongly on the season, time of day, and satellite location. A large number of satellite-based precipitation products have been designed using different spectral channels, which are combined with other data, most commonly microwave active data from ground-based and satellite radars (e.g. Global Precipitation Measurement (GPM)), microwave passive data from satellites in low polar orbits (e.g. MetOp of the National Oceanic and Atmospheric Administration (NOAA)), and mesoscale numerical model forecasts. This created the need for several comparative studies that were carried out in Europe, despite their much lower usefulness here (see, for example, Jiang et al., 2019; Navarro et al., 2020; Tapiador et al., 2020; Mahmoud et al., 2021; Peinó et al., 2025).

Additionally, precipitation data may come from devices not originally designed for meteorological measurements. The most common instance uses signal attenuation measurements on commercial microwave links (CMLs) from mobile phone networks (van der Valk et al., 2024; Olsson et al., 2025). These data require sophisticated algorithms to convert the measurements to precipitation, but they can provide many times more data than rain gauge networks. In Europe, attempts are being made to use these data in real time (Overeem et al., 2016; Nielsen et al., 2024; Graf et al., 2020, 2024; Olsson et al., 2025), taking advantage of the fact that networks with these kinds of links are very dense, especially in urbanised areas.

# 1.2.2 Multi-source estimates

None of the measurement techniques described above demonstrates the ability to provide accurate precipitation estimation individually, but they are largely complementary. Considering that each has advantages and disadvantages, the idea is to combine data from different sources to improve the accuracy of rainfall estimation while maintaining a high spatial resolution. Consequently, several merging methods have been developed to address the strengths and limitations of each measurement technique. They often include approaches based on conditional combinations of individual data (e.g. Sinclair and Pegram, 2005; Jurczyk et al., 2020b); the Kalman filter; and various versions of Kriging, such as Kriging with external drift (Sideris et al., 2014). Machine learning techniques, such as XGBoost (Mai et al., 2022; Putra et al., 2024), have been increasingly used for this purpose. Most often the merging process involves data from rain gauge and radar techniques (e.g. Goudenhoofdt and Delobbe, 2009; Ochoa-Rodriguez et al., 2019; Wijayarathne et al., 2020) and less often from the three combined techniques of rain gauge, radar, and satellite (e.g. Jurczyk et al., 2020b; Yu et al., 2020; Putra et al., 2024). NOAA operationally provides the Multi-Radar Multi-Sensor (MRMS) quantitative precipitation estimates generated through the integration of data from radar networks, surface and satellite observations, numerical weather prediction (NWP) models, and climatology (Zhang et al., 2016).

#### 1.2.3 Estimates based on numerical models

The surface or near-surface fields of precipitation simulated by NWP models are now frequently used for various purposes, including the research of extreme precipitation events (Bližňák et al., 2022). Atmospheric reanalyses produced by NWP models with the assimilation of available historical observations can reconstruct past meteorological conditions. They provide physically consistent datasets of variables, including surface precipitation (Hersbach et al., 2020). The current NWP models are able to simulate intense precipitation, but the agreement with rain gauge observations is still not high in terms of the spatial and temporal representation of precipitation (Bližňák et al., 2019).

For the characterisation of precipitation patterns, it is possible to use precipitation simulations obtained from NWP models, such as the publicly available ERA5 of ECMWF reanalyses (e.g. Subba et al., 2024). Other high-resolution mesoscale models with open-access software, such as Weather Research and Forecasting (WRF) of NCAR (Tanessong et al., 2017; Skamarock et al., 2019), can also be used. A significant upside to using such a solution, even in areas with dense in situ measurement networks, is the easy access to the data and their convenient processing.

# 1.2.4 Problems in the verification of precipitation measurements

Although several methods for verifying precipitation data have been developed over the years (e.g. Rodwell et al., 2011; Szturc et al., 2022), this issue is still challenging (Skok, 2022; Zhang et al., 2025). A fundamental problem in precipitation measurements is the considerable difficulty deriving information about precipitation on the ground surface, the so-called ground truth. Therefore, empirical verification of different measurement or estimation techniques is generally carried out indirectly through their intercomparison during field experiments. This process often involves a somewhat arbitrary selection of the most reliable measurement data or estimates based on the experience of the researchers. Rain gauges, especially manual ones, are believed to provide direct and relatively accurate data from point rainfall measurements. Thus, they are often considered the ground truth source for verifying other, mostly grid-based rainfall products, such as radar- and satellite-based, multi-source, or NWP model reanalyses (e.g. Militino et al., 2018). In a very sparse network of manual rain gauges, telemetric rain gauges can be used for this purpose but only after advanced quality control.

The problem of precipitation data verification is much more difficult in mountainous areas due to the more significant spatial variability of precipitation distribution, which is associated with complex terrain (Ouyang et al., 2021). This aspect should also be kept in mind when verifying different types of measurements (Merino et al., 2021).

Furthermore, comparing the average precipitation over a grid area to a specific point value introduces some uncertainty, particularly during heavy rain (Ensor and Robeson, 2008). An analysis of findings by Sun et al. (2018), Herrera et al. (2019), and others shows that, due to the high spatial variability of precipitation, it is not possible to establish a single universal error value when comparing point and grid data. The level of the uncertainty varies depending on the nature of the precipitation. For widespread (large-scale) precipitation, the uncertainty typically ranges from about 10 % to 15 %. However, for intense convective extreme precipitation, this uncertainty can rise to approximately 15 % to 25 % (Schellart et al., 2017; Henn et al., 2018; Tarek et al., 2021). Special care should be taken when analysing local precipitation maxima using gridded data, as noted by Sun et al. (2018) and others, who point out that these data may smooth out extreme values compared to point measurements.

# 1.3 Objectives and structure of the paper

The main objective of this work is to examine the real possibilities of precise estimation of a precipitation field with a high spatial resolution of about 1 km and a high temporal resolution of at least 10 min or 1 h during the intense precipitation events that caused floods in the upper Odra River basin area in September 2024. All available real-time and offline measurements and estimates were verified to determine their applicability and to quantify their reliability.

The paper is organised as follows: after the introductory Sect. 1 outlining the issues of precipitation measurement and the various techniques used, Sect. 2 briefly describes the 2024 flood event and the area affected. Section 3 details the precipitation data used in this work, available both in real time and with a delay for a longer period. Section 4 presents the results of the statistical verification of the data obtained by the different techniques and outcomes of the comparative analyses. Section 5 provides conclusions drawn from evaluating the reliability of the investigated measurements and estimates.

#### 2 Flood in Poland in the Odra River basin in 2024

#### 2.1 Characteristics of the flooded area

The Odra (or Oder) is the second-largest river in Poland. It forms part of the central European drainage network. The river starts in the Sudety Mountains in the Czech Republic and flows north, mainly through Polish territory, to the Baltic Sea. The river's total length is 855 km, and the maximum el-

evation in its basin is 1602 m above sea level (a.s.l.) in the Sudety (Mount Śnieżka). After the Carpathian Mountains, the Sudety Mountains have Poland's highest annual precipitation accumulation. At the same time, the area is characterised by high precipitation variability due to the complex orography, the natural increase in precipitation intensity with altitude, and the occurrence of precipitation shadows in the lower parts of the mountains and valleys.

The rivers draining the Sudety Mountains and the foothills are prone to dangerous floods that can occur after high precipitation. The Odra River basin is characterised by numerous left-bank short tributaries draining rainwater from the mountains. Moreover, in the case of the Kłodzko Valley, there is a concentric system of river networks that favours the occurrence and dynamic of flood phenomena (e.g. Szalińska et al., 2014; Ligenza et al., 2021).

Rain-induced floods in the Odra River basin are usually associated with low-pressure frontal centres that reach Poland and cause prolonged and intense precipitation in the south of the country. In Poland, catastrophic rainfall floods occur most frequently in the upper and middle Odra basin only, with an area of approximately 44 000 km<sup>2</sup> (Fig. 1), on average every 10–15 years. The last ones were recorded in 1997, 2010, and 2024, the latter of which was investigated in this study.

The literature on analysing these floods is extensive, generally in Polish, but comprehensive English-language scientific studies can also be found. They address the subject from very different perspectives. Some studies cover a wider area than the Odra basin, e.g. the whole of Poland (e.g. Kundzewicz, 2014), central and eastern Europe (Bissolli et al., 2011), or the whole of central Europe (Mudelsee et al., 2004; Kimutai et al., 2024). Others describe and analyse in detail the course of floods (precipitation and river flows) in specific basins, e.g. the Odra River in Poland (Szalińska et al., 2014) or the Nysa Kłodzka River (Perz et al., 2023), which is an important tributary of the Odra River. Research suggests that climate change affects the frequency and severity of floods, leading to an increased risk of flooding (e.g. Kundzewicz et al., 2023). Detailed statistical analyses of rainfall during floods have also been carried out (e.g. Mikolajewski et al., 2025).

The above studies indicate that the upper Odra River basin is highly vulnerable to flooding caused by intense precipitation in the mountainous part of the basin. This is also influenced by the shape of the river network, which favours the cumulation of floods from individual tributaries. The flood risk there occurs almost annually during the summer.

# 2.2 Description of the flood

On 12–15 September 2024, the upper and middle Odra River basin and part of the upper Vistula River basin experienced rainfall that significantly changed the hydrological situation. From 12 September 2024, intense rainfall began to appear in western Poland, with accumulations of up to 60 mm in

12 h recorded in the eastern Sudety Mountains. The highest rainfall intensity occurred on consecutive days: from 13 September in the morning to 15 September 2024 before noon. The precipitation was associated with a low-pressure system, named Boris by the national meteorological services of southern and central Europe.

At many locations, the daily precipitation accumulation in this period exceeded 200 mm, and its territorial range covered mainly the eastern Sudety Mountains. Four-day precipitation accumulation reached values above 400 mm, with the highest in the Jeseníky and Śnieżnik mountains. They might have exceeded even 550 mm, as indicated by reanalyses RainGRS Clim (Jurczyk et al., 2023) based on estimates from the RainGRS system and adjusted to observations from manual rain gauges (Fig. 2). Apart from intense, widespread precipitation, numerous thunderstorms and several associated tornadoes were recorded during these days. On 16 September, rainfall began to diminish; mainly light to moderate precipitation was observed, and in the following days, the weather in Poland was influenced by a highpressure system, with the advection of warm and dry air of continental origin.

The consequence of the intensive rainfall was the runoff of rainwater, high and extreme water levels in rivers, and flooding. The flood wave moved down the Odra River and its tributaries, causing numerous exceedances of warning and alarm levels.

### 3 Data used for flood monitoring and analyses

#### 3.1 The data used

In the frame of this study, the input data used to retrieve the precipitation field (Table 1) are divided into two groups in terms of the delay in their availability: (i) in real time and near real time and (ii) not in real time (with a delay of more than 30 min). Among the latter, data from manual rain gauges (GAU Manual), characterised by the highest reliability based on knowledge of measurement techniques and experience, were selected as reference data. All other precipitation products are verified by a quantitative comparison with them.

#### 3.2 Operational data available in real time

All measurement data require quality control (QC) that employs adequately designed systems, which are often very sophisticated (Szturc et al., 2022), especially for weather radar data. These systems are dedicated to verifying the data and, if necessary, correcting them. Using different precipitation information and a cross-check approach in a QC scheme is a common practice.

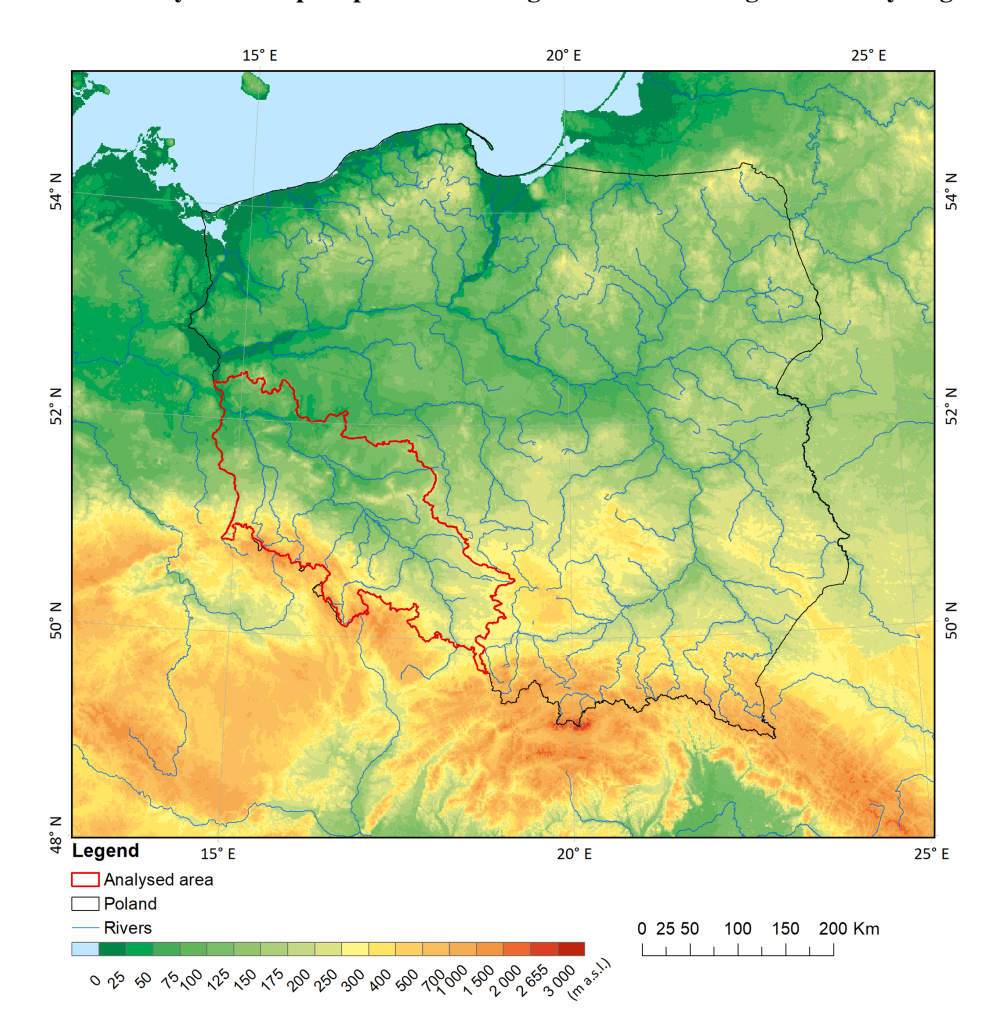
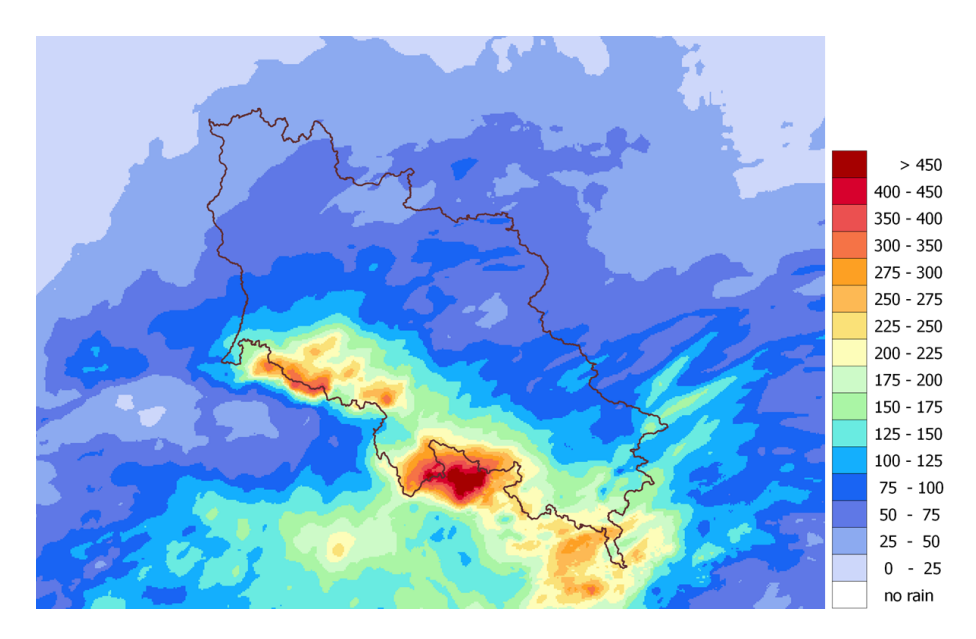


Figure 1. The area of the upper and middle Odra River basin in Poland.



**Figure 2.** Field of precipitation accumulation during the flood of 13–16 September 2024 (4 d) for the upper and middle Odra River basin in Poland, obtained from the multi-source RainGRS Clim estimates.

Abbreviation	Description	Temporal resolution	Spatial resolution	Timeliness
Reference data				
GAU Manual	Data from manual rain gauges (Hellmann type)	24 h	Point-wise	2 months
Data available i	n real time			
GAU	Interpolated data from telemetric rain gauges	10 min	1.0 km	6 min
RAD	Weather radar data from POLRAD and neighbouring countries	5/10 min	0.5/1.0 km	4 min
RAD Adj	Weather radar data from POLRAD and neighbouring countries adjusted to telemetric rain gauge data	5/10 min	0.5/1.0 km	7 min
SAT	Satellite-based precipitation – combination of EUMETSAT NWC SAF products	5/10 min	Roughly $3.5 \text{ km} \times 6.0 \text{ km}^*$	4 min
H61B	Satellite-based precipitation – MW-IR combination (EUMETSAT H SAF product)	1, 24 h	Roughly $3.5 \text{ km} \times 6.0 \text{ km}^*$	5–10 min
CML	Interpolated estimates based on signal attenuation in commercial microwave links	15 min	1.0 km	Tests in progress (currently offline)
GRS	Multi-source estimates from RainGRS system	10 min	1.0 km	7 min
Data available 1	not in real time (offline)			
IMERG	Satellite-based precipitation estimates of NASA, final analyses (IMERG Final)	30 min	Roughly $7 \text{ km} \times 11 \text{ km}^*$ $(0.1^{\circ} \times 0.1^{\circ})$	About 4 months
PDIR-Now	Satellite-based precipitation estimates of University of California, Irvine	1 h	Roughly $2.8 \text{ km} \times 4.5 \text{ km}^*$ $(0.04^{\circ} \times 0.04^{\circ})$	30–60 min
ERA5	ECMWF reanalyses (NWP-based estimates)	1 h	Roughly $18 \text{ km} \times 28 \text{ km}^*$ $(0.25^{\circ} \times 0.25^{\circ})$	5 d
WRF	WRF reanalyses (with initial conditions from ICON model)	1 h	1.0 km (settable)	4.5 h

<sup>\*</sup> In the area of the study basin.

# 3.2.1 Rain gauge measurements

The network of telemetric rain gauges of the Institute of Meteorology and Water Management – National Research Institute (IMGW) – the NMHS in Poland – consists of about 650 stations, mainly of the tipping bucket type. There are 158 stations in the area analysed in this work (Fig. 3), which gives an average of one rain gauge per approximately  $280\,\mathrm{km}^2$ . This network is much denser in the mountains, including the Sudety Mountains, than in other parts of the country, with one station per approximately  $420\,\mathrm{km}^2$ .

Precipitation measurements are transmitted in the form of 10 min accumulations. Additionally, analogous data from the Czech Republic (CHMU – the Czech NMHS) from gauges

near the Polish border are also operationally available. All data are subject to quality control by the RainGaugeQC system developed at IMGW (Ośródka et al., 2022, 2025). The point measurements are interpolated using the ordinary Kriging method to obtain a precipitation field with a 1 km resolution.

#### 3.2.2 Weather radar measurements

POLRAD, IMGW's weather radar network, consists of 10 C-band, Doppler, and polarimetric radars manufactured by Leonardo Germany. The network is supplemented by data from 10 radars from neighbouring countries, whose observations partially cover the territory of Poland (Fig. 3). The

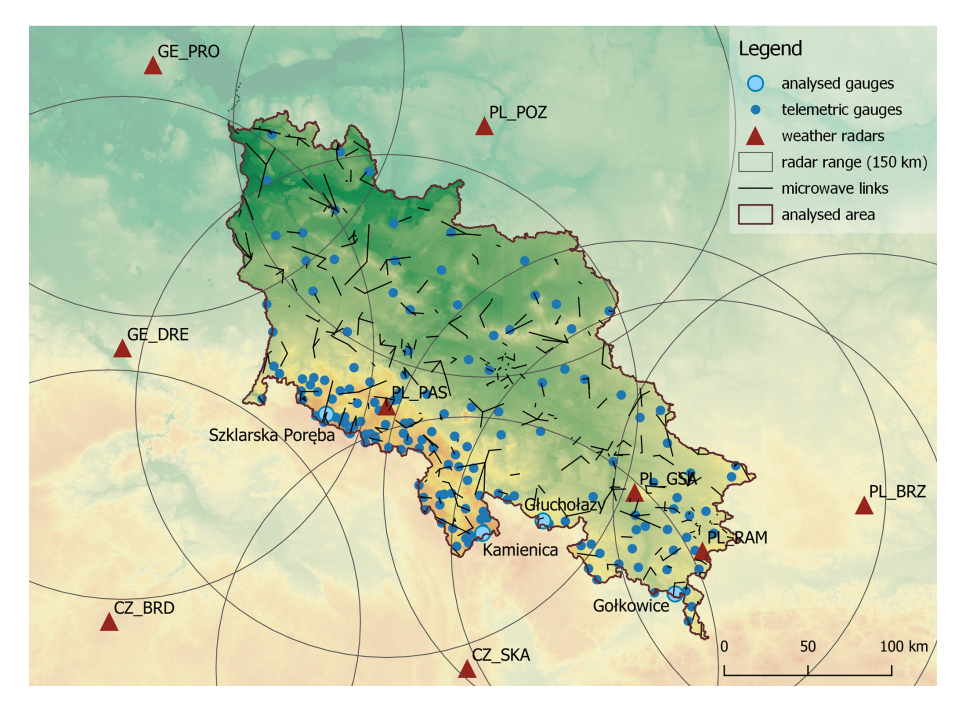


**Figure 3.** Locations of measurement stations in the upper and middle Odra River basin: telemetric rain gauges (blue dots), weather radars (brown triangles) with 150 km range (brown circles), commercial microwave links (black lines), and four manual rain gauges selected for more detailed analysis (larger blue dots).

radar data are quality controlled with the RADVOL-QC system designed at IMGW (Ośródka et al., 2014; Ośródka and Szturc, 2022). The precipitation composite maps are generated based on the PseudoSRI products from individual radars with a merging algorithm that considers a combination of data quality information and distance from the radar site (this was also developed at IMGW; Jurczyk et al., 2020a). The spatial resolution of the final field is  $1 \, \mathrm{km} \times 1 \, \mathrm{km}$ , and the temporal resolution is  $10 \, \mathrm{min}$ .

However, it should be noted that radar estimates of precipitation in mountainous areas are usually less reliable due to disturbances arising from the interaction of the radar beam with the terrain. Therefore, algorithms for the adjustment of radar-based precipitation with rain gauges are becoming more important. A mean field bias correction is carried out individually for each radar based on a 10 min accumulation. Then, the spatial adjustment is performed based on a comparison of past radar estimates with corresponding rain gauge data to handle non-uniform bias within the radar composite domain (Jurczyk, 2020b).

The flooding area is within the range of five Polish radars, three located in the upper and middle Odra River basin: Pastewnik (PL\_PAS), Góra św. Anny (PL\_GSA), and Ramża (PL\_RAM); and, in its vicinity, Poznan (PL\_POZ) and Brzuchania (PL\_BRZ). Moreover, two German radars, Protzel (GE\_PRO) and Dresden (GE\_DRE), and one Czech radar, Skalky (CZ\_SKA), partially cover the basin area.

#### 3.2.3 Satellite measurements and estimations

Satellite precipitation fields for Europe are based primarily on data from geostationary meteorological satellites of the Meteosat family, which are positioned over the Equator at various longitudes. They are an important source of operational data due to their very high temporal resolution of 5 min and quick access of a few minutes. Their spatial resolution, which for the area of southern Poland is approximately  $3.5~{\rm km} \times 6.0~{\rm km}$ , is also relatively high in terms of satellite data.

Depending on the availability of additional data, it is possible to generate different satellite-based estimates in real time or in near real time, such as precipitation fields based on products generated by software developed by EUMETSAT programmes. IMGW operationally uses products generated by the software of the EUMETSAT (2021) programme from the visible (daytime CRR-Ph and PC-Ph products) and infrared (24 h CRR and PC) data. On this basis, 10 min precipitation accumulation fields are estimated by IMGW software (Jurczyk et al., 2020b). These data are corrected by mean field bias, with radar precipitation adjusted to rain gauge measurements. The H61B precipitation product of the EU-METSAT (2020) programme is also available, which, unlike the SAT product, is based only on data from the IR channel available 24 h a day but is supplemented with observations from passive microwave sensors located on various meteorological satellites in low polar orbits.

#### 3.2.4 Other estimates

Measurements of signal attenuation on commercial microwave links (CMLs) allow the calculation of the integrated precipitation along a given link, with a length of several to tens of kilometres (Olsson et al., 2025). The precipitation is spatially distributed along the link in proportion to the distribution of weather radar (RAD) precipitation along this distance (Pasierb et al., 2024). There are 400 such links in the area analysed in this study (Fig. 3), which gives an average of one link per around 100 km<sup>2</sup>.

The CML-based 15 min precipitation accumulations are spatially interpolated using inverse distance methods to obtain high-resolution  $1 \text{ km} \times 1 \text{ km}$  precipitation fields. The data are currently being tested at IMGW for their applicability to real-time operational applications.

#### 3.2.5 Multi-source estimates

The RainGRS model, combining rain gauge, radar, and satellite precipitation data, is used operationally at IMGW (Jurczyk et al., 2020b), applying a conditional merging technique that is a development of the Sinclair and Pegram (2005) algorithm. This method is enhanced by involving detailed quality information assigned to individual input data. The combination algorithm is divided into two stages. At first, rain gauge data are merged with radar and satellite estimates separately, taking into account their quality. Finally, the resulting two precipitation fields are combined using weights, depending on the distance from the nearest radar site and the quality of the satellite precipitation. As a result, a multi-source gauge–radar–satellite (GRS) field is received, with a spatial resolution of 1 km × 1 km and a temporal resolution of 10 min.

# 3.3 Estimates not available in real time

# 3.3.1 Manual rain gauge measurements

The IMGW network of manual rain gauges consists of about 641 stations. Their operation involves employing a graduated cylinder from which the observer reads the height of the rainwater column. In Poland, such gauges are used in the Hellmann standard; however, their measurements have some limitations: (i) they are point-wise, (ii) they have relatively long precipitation accumulation times of, most often, 24 h, and (iii) they require measurement processing (including quality control), so they are not available in real time. The data from manual rain gauges are the closest to reality at their locations and therefore were selected as the point reference for the 2024 flood. There are 112 such stations in the area analysed in this study (Fig. 4): one rain gauge per approximately 395 km<sup>2</sup>.

# 3.3.2 Satellite-based reanalyses

Satellite-based reanalyses use additional information, especially from satellites on polar low-Earth orbits, beyond what is available from geostationary satellites, and this improves their reliability. However, this requires more time to acquire and process data, so the delay in access to the estimates in such cases can be as long as several months (Berthomier and Perier, 2023).

The Integrated Multi-satellitE Retrievals for GPM (IMERG) is a NASA product estimating global surface precipitation rates at a spatial and temporal resolution of  $0.1^{\circ} \times 0.1^{\circ}$  and 30 min, respectively (NASA, 2025). This product is calibrated with Global Precipitation Measurement (GPM Core Observatory) satellite data, which is based on a microwave imager and the dual-frequency precipitation radar, and uses it as a baseline. This is combined with other observations from national or international satellite constellations equipped with weather radars and passive microwave and infrared sensors, as well as with rain gauge data (Huffman et al., 2020; Bogerd et al., 2021). IMERG has three runs with different delays: Early Run (4 h delay), Late Run (14 h), and Final Run (about 4 months).

The PERSIANN Dynamic Infrared Rain Rate Near Real-Time (PDIR-Now) is a global high-resolution  $(0.04^{\circ} \times 0.04^{\circ})$  satellite-based precipitation estimation product developed by the University of California, Irvine (UCI) (Nguyen et al., 2020a, b; Afzali Gorooh et al., 2022; CHRS, 2025). It is based on the high-frequency sampling of infrared imagery and has a timeliness of 30–60 min. PDIR-Now considers errors due to the use of IR imagery by applying various techniques, including dynamic curve shifting (Tb-R) based on precipitation climatology. Its highest temporal resolution is 1 h.

# 3.3.3 Reanalyses of the NWP models

The ERA5 fields (ECMWF Reanalysis v5) generated by the European Centre for Medium-Range Weather Forecasts (ECMWF) have a low resolution of  $0.25^{\circ} \times 0.25^{\circ}$ , which, once converted to distance units, correspond to grids of approximately  $18 \, \text{km} \times 26 \, \text{km}$  in Poland (ECMWF, 2025). Such data allow for an overall analysis of rainfall offline. However, it is impossible to use these reanalyses when knowledge of the course of convective phenomena at the microscale is needed, i.e. with a spatial resolution of  $1 \, \text{km}$  or less.

The Weather Research and Forecasting (WRF) is a model developed at the National Center for Atmospheric Research (NCAR, 2025). Initial conditions for simulations of precipitation during the flood analysed here were taken from the ICON-EU (Icosahedral Nonhydrostatic) model (6.5 km) developed at Deutscher Wetterdienst (German NMS, DWD, 2025). Simulations were conducted at 50 vertical levels up to 50 hPa, with a horizontal resolution of 1 km and a time

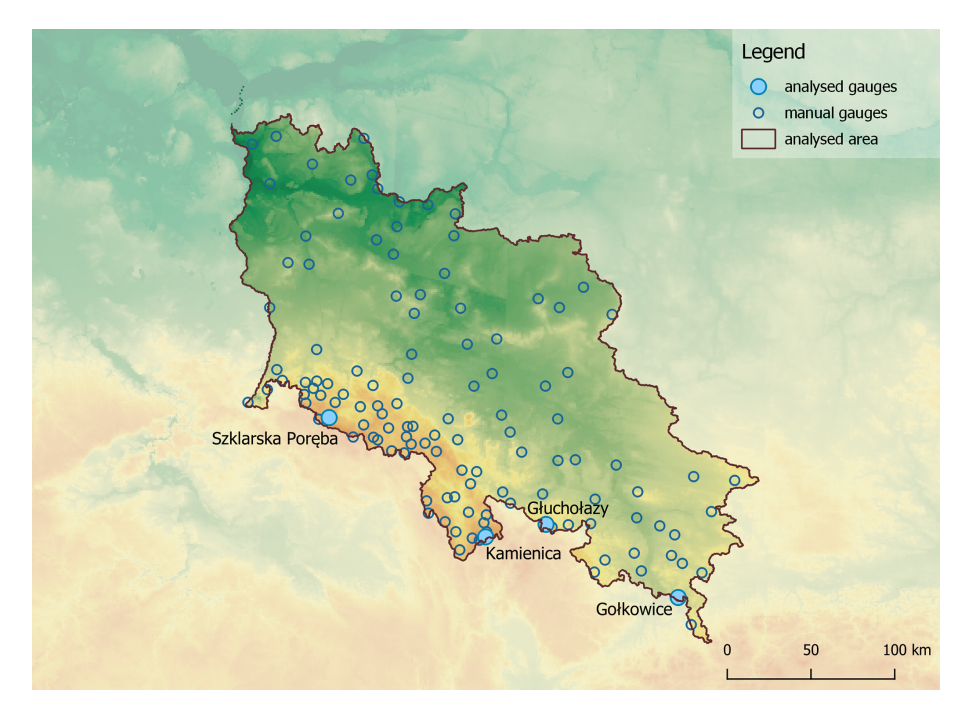


Figure 4. Locations of manual rain gauges (blue circles) and four ones selected for more detailed analysis (larger blue dots) in the upper and middle Odra River basin.

step of 1 h. Thompson's microphysics scheme (Thompson et al., 2004) was utilised in the simulations. Due to the high resolution of the computational domain, explicit wet process physics was implemented, along with the parameterisation of shortwave and longwave radiation based on the RRTMG radiation propagation scheme, a newer version of RRTM (Iacono et al., 2008). Boundary layer processes were modelled according to the Mellor–Yamada–Nakanishi–Niino (MYNN) turbulence scheme with closure 2.5 (Nakanishi and Niino, 2009). The near-surface layer was parameterised using the MYNN scheme (Nakanishi and Niino, 2006). The multi-physics Noah land surface model (Niu et al., 2011) predicts soil moisture and temperature at four depths (Jarvis, 1976).

# 4 Reliability analysis of different techniques of precipitation measurement and estimation

# 4.1 Methodology for verifying precipitation data

The basic analyses were carried out for 1 d accumulations with reference data from manual rain gauges (GAU Manual), which we consider to be the most reliable values. These measurements are point-wise, so the verification of individual precipitation fields was performed only at the locations of these stations (112 ones). The data were from 13–16 September 2024, but at IMGW, measurements of meteorological daily precipitation are made at 06:00 UTC, i.e. the accumulation for a given day is summed from 06:00 UTC of the

previous day to 06:00 UTC of the following day and assigned to the date on which the accumulation ended. Thus, the period analysed included precipitation from 06:00 UTC on 12 September to 06:00 UTC on 16 September.

The temporal distribution of heavy precipitation plays a key role, so the data available with a 1 h time step were also verified. As measurements from manual rain gauges are not available at such a short time step, the RainGRS (GRS) fields (44 218 pixels within the basin) were used as a benchmark for the verification. In this case, it was possible to conduct a spatial verification because the reference was data with a resolution of  $1 \text{ km} \times 1 \text{ km}$ . However, it should be noted that the GRS estimates depend on some of the verified data (GAU, RAD, RAD Adj, and SAT).

The following metrics were employed:

 The Pearson correlation coefficient is a well-known metric that is sensitive to a linear relationship between two datasets and reflects agreement between estimate and reference in terms of spatial pattern:

$$CC = \frac{\sum_{i=1}^{n} (E_i - \overline{E}) (O_i - \overline{O})}{\sqrt{\sum_{i=1}^{n} (O_i - \overline{O})^2 \sum_{i=1}^{n} (E_i - \overline{E})^2}}.$$
 (1)

 Root mean square error based on variance is a standard metric used in verification studies as a good measure of differences between the verified and reference values:

RMSE = 
$$\sqrt{\frac{1}{n} \sum_{i=1}^{n} (E_i - O_i)^2}$$
. (2)

The RMSE is particularly sensitive to outliers as squaring the errors emphasises larger deviations.

 Root relative square error is similar to the RMSE, but it is scale independent as it relates the deviations to the spread of the reference values around their mean:

RRSE = 
$$\frac{\sqrt{\sum_{i=1}^{n} (E_i - O_i)^2}}{\sqrt{\sum_{i=1}^{n} (O_i - \overline{O})^2}}.$$
 (3)

- Statistical bias is a measure of systematic error:

Bias = 
$$\frac{1}{n} \sum_{i=1}^{n} (E_i - O_i)$$
, (4)

where  $E_i$  is the estimated value,  $O_i$  is the reference value, i is the gauge/pixel number, and n is the number of gauges/pixels, whereas  $\overline{E}$  and  $\overline{O}$  are the mean values of  $E_i$  and  $O_i$ , respectively.

# **4.2** Precipitation fields obtained from various measurement techniques and estimation methods

The daily precipitation accumulations for the flood event of 13–16 September 2024, derived from various measurement techniques and estimation methods described in this paper (Table 1), are presented below. These include (i) reference data from spatially interpolated manual rain gauge observations (Fig. 5), (ii) precipitation fields operationally available in real time (Fig. 6), and (iii) offline reanalyses (Fig. 7).

A visual assessment of the differences between all the verified data and the reference allows the following general observations to be formulated.

The GAU and multi-source GRS rain gauge fields accurately reproduce the spatial distribution of the precipitation field and are consistent with the reference in terms of values. Differences are visible mainly in the Karkonosze Mountains on the border with the Czech Republic, probably due to the densities of the GAU Manual and GAU networks (the latter is higher in this area) and the influence of data from the Czech territory.

In the case of radar-derived fields (RAD and RAD Adj), the precipitation pattern is also well represented, but the estimates based solely on radar observations (RAD) underestimate values. Therefore, unadjusted radar data should not be used, especially for quantitative precipitation estimates (WMO, 2025). Radar data after adjustment with rain gauge

measurements (RAD Adj) demonstrate good agreement concerning precipitation values. The radar network in the analysed flood area is relatively dense, but due to signal blocking by mountains, precipitation shadows appear in some places, which result in an underestimation of precipitation. This is particularly evident in the Kłodzko Valley, which is surrounded by relatively high mountains and is one of the places most prone to catastrophic flooding.

Estimates generated based on satellite data – SAT, H61B, and PDIR-Now – reproduce the precipitation distribution in space very imprecisely, and values are significantly lower than the reference. The IMERG reanalysis definitely represents the precipitation field better, but values are also underestimated, especially in places where accumulations are highest. The reliability of precipitation estimates based on satellite data is low, especially when they are generated from infrared channel data and are not supported by other, preferably microwave, data (from radars). This mainly affects SAT estimates but also others. It should be noted that during the analysed flood, data from visible channels were only available for about one-third of the time, due to the fact that for the measurements to be reliable, the sun must be sufficiently high above the horizon (above 20 degrees). Furthermore, the spatial resolution of these data is generally insufficient.

The CML-based estimates represent precipitation variability quite correctly, but the values compared to the reference are slightly lower. It can be clearly seen that spatial representativity is limited due to the lower density of the links in the higher parts of the mountains, such as in the eastern part of the Kłodzko Valley.

Estimates based on numerical mesoscale models (ERA5 and WRF) correctly reproduce the precipitation pattern. However, the ERA5 reanalyses have a very low spatial resolution, so they do not reflect the fine-scale structures of the precipitation field, and, in addition, the values are more underestimated than those derived from WRF simulations.

# 4.3 Verification of daily and hourly precipitation accumulations

Daily precipitation accumulations derived from different measurement techniques and estimations, listed in Table 1, were verified against point-wise observations from manual rain gauges. Table 2 summarises the values of the characteristics defined in Sect. 4.1 and, additionally, the relationship between CC and RMSE values for the verified measurement techniques is shown in the graph in Fig. 8.

Most of the analysed data estimate precipitation correctly, in particular the GAU, RAD Adj, and GRS fields, which exhibit an extremely high correlation coefficient (CC > 0.9); the differences between verified and reference values are very low, taking into account the magnitude of the rainfall (RMSE < 15 mm). Therefore, these fields can correctly represent precipitation with high spatial resolution for operational purposes and subsequent analyses.

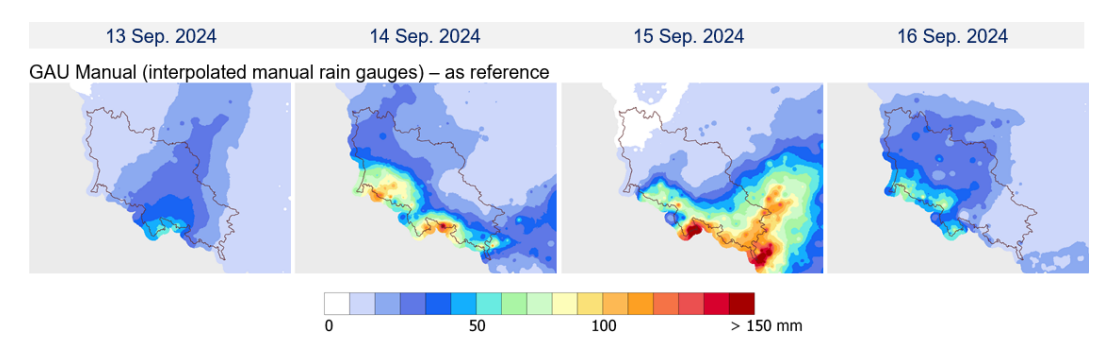


Figure 5. Reference fields from manual rain gauges for daily precipitation accumulations from 13 to 16 September 2024. Data are limited to the upper and middle Odra River basin area.

**Table 2.** Values of statistics for daily precipitation accumulations from 13 to 16 September 2024 against data from manual rain gauges (GAU Manual) as reference.

Measurement/ estimation technique	Mean (mm)	CC (-)	RMSE (mm)	RRSE (-)	Bias (mm)			
Reference data								
GAU Manual	41.78	_	_	-	_			
Available in rea	l time							
GAU	38.27	0.963	10.40	0.29	-3.50			
RAD	16.07	0.784	38.08	1.06	-25.71			
RAD Adj	36.65	0.956	12.42	0.35	-5.13			
SAT	10.02	0.395	46.06	1.28	-31.76			
H61B	18.77	0.455	39.46	1.10	-23.00			
CML	21.13	0.721	32.74	0.91	-20.65			
GRS	37.94	0.967	10.02	0.28	-3.83			
Available offline								
IMERG	27.15	0.552	33.40	0.93	-14.63			
PDIR-Now	20.23	0.138	42.57	1.18	-21.55			
ERA5	32.63	0.748	26.00	0.72	-9.15			
WRF	30.48	0.759	26.02	0.72	-11.30			

The ERA5 and WRF simulations performed slightly worse, with CC above 0.7, which suggests quite good agreement with the reference, but the RMSE is already high – above 25 mm. WRF reanalyses turned out better, with CC=0.77 and RMSE=25.6 mm. In the case of the RAD and CML fields, the correlation coefficient is also high (CC>0.7), but a significant underestimation of precipitation is evident, as indicated by large RMSE values > 30 mm, with Bias of -25.7 and -20.6, respectively.

The worst results were obtained for the satellite-based estimates: SAT, H61B, and PDIR-Now, for which CC < 0.5 and RMSE > 35 mm, and only slightly better statistics were achieved for the IMERG estimates (CC = 0.55, RMSE = 33.4 mm).

**Table 3.** Values of statistics for hourly precipitation accumulations from 13 to 16 September 2024 against the RainGRS estimates (GRS) as reference.

Measurement/ estimation	Mean (mm)	CC (-)	RMSE (mm)	RRSE (-)	Bias (mm)
Reference data					
GRS	1.05	_	_	_	_
Available in real time					
GAU (dependent)	1.03	0.906	0.60	0.41	-0.01
RAD (dependent)	0.49	0.902	1.07	0.70	-0.56
RAD Adj (dependent)	1.03	0.977	0.29	0.22	-0.01
SAT (dependent)	0.33	0.256	1.75	1.21	-0.72
H61B	0.61	0.174	1.70	1.21	-0.44
CML	0.60	0.673	1.11	0.83	-0.45
Available offline					
IMERG	0.94	0.529	1.39	0.98	-0.11
PDIR-Now	0.70	0.114	1.89	1.45	-0.35
ERA5	1.11	0.497	1.34	0.93	0.06
WRF	0.94	0.367	1.67	1.20	-0.10

Further research was conducted to evaluate the usefulness of the investigated data at a higher temporal resolution – hourly instead of daily. Table 3 shows results analogous to those depicted in Table 2, but the reference in this case are the RainGRS estimates (GRS fields), as measurements from manual rain gauges are only available as daily accumulations. These data were selected as a benchmark because the correlation between the two fields (i.e. GAU Manual and GRS) for daily accumulations is the best, being as high as 0.97, and Bias is as low as  $-3.8 \, \text{mm}$  (Table 2). The relationship between the CC and RMSE values for the verified measurement techniques is shown in the graph in Fig. 9.

In terms of the much higher temporal resolution of the measurements and estimates, fewer of them maintain a corresponding high reliability. Both the GAU and RAD Adj estimates demonstrated excellent results, with CC values exceeding 0.9 and RMSE values of 0.6 and 0.3 mm, respec-

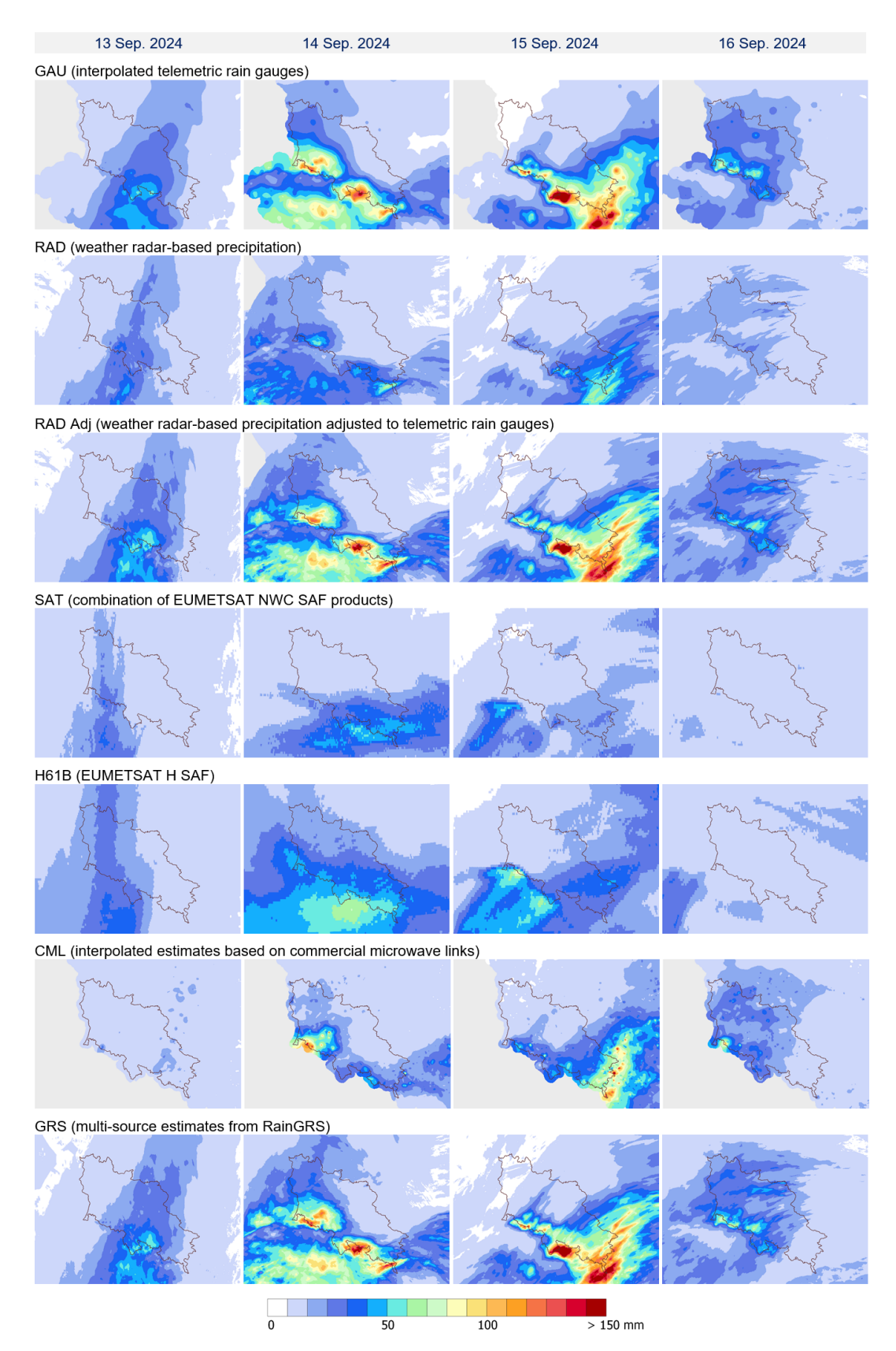


**Figure 6.** Precipitation fields available in real time for daily precipitation accumulations from 13 to 16 September 2024. Data are limited to the upper and middle Odra River basin area.

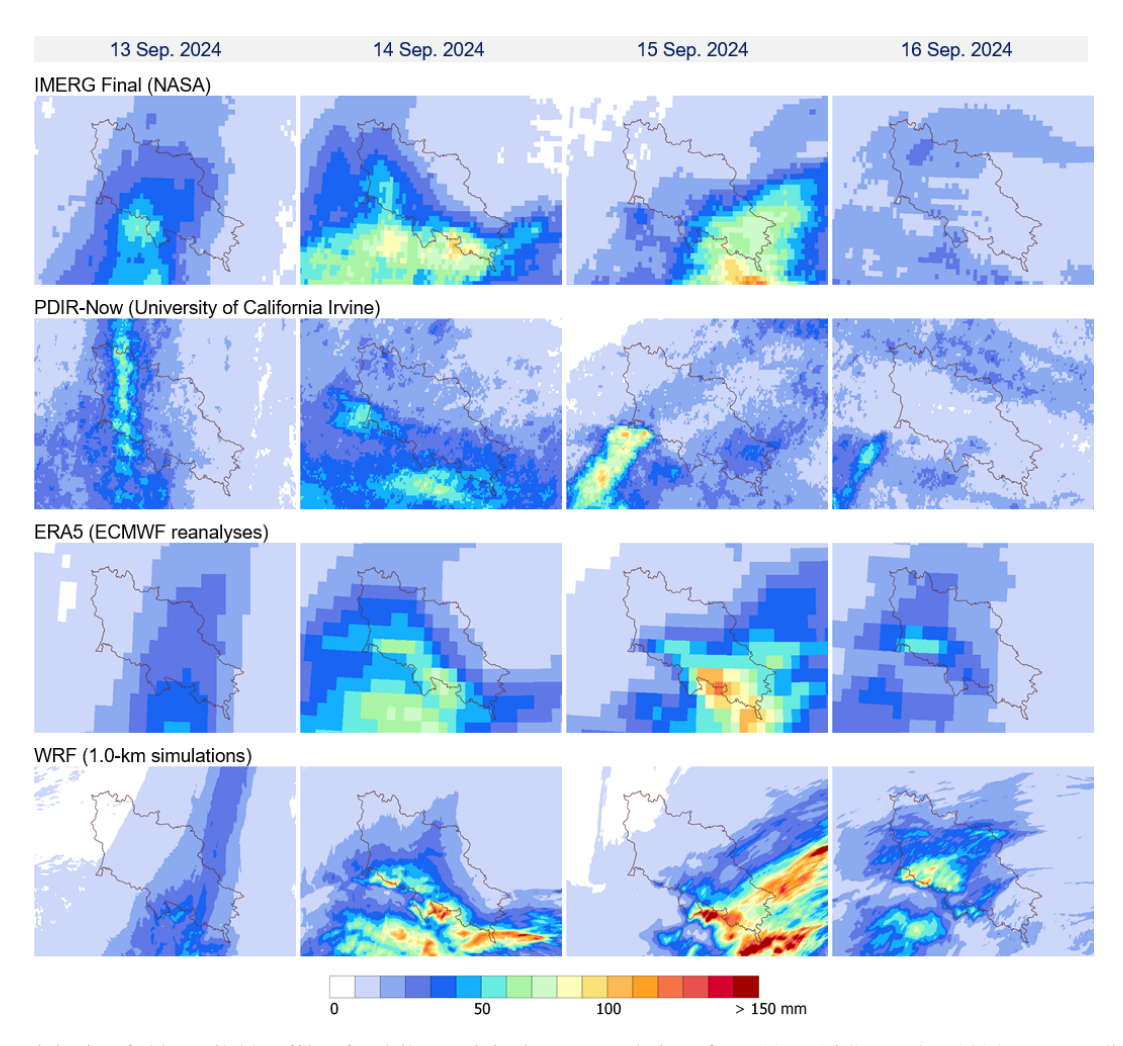
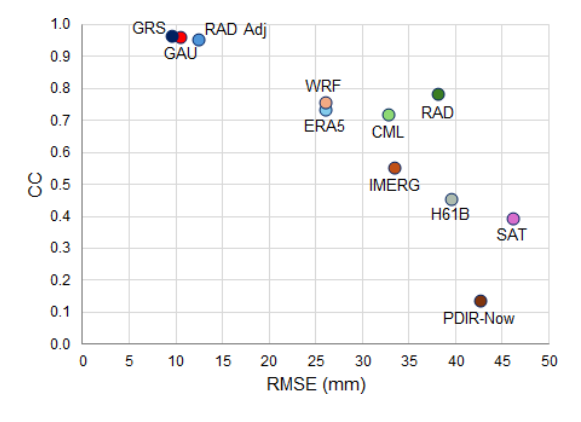
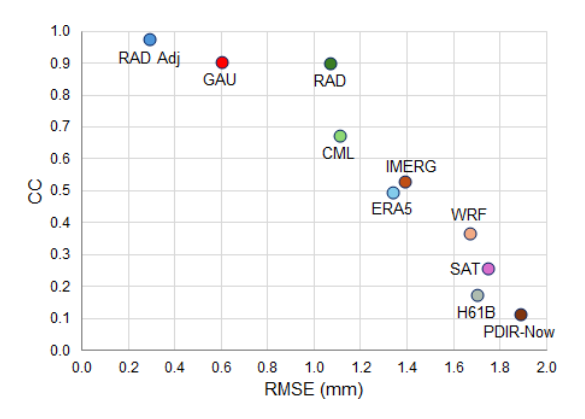


Figure 7. Precipitation fields available offline for daily precipitation accumulations from 13 to 16 September 2024. Data are limited to the upper and middle Odra River basin area.



**Figure 8.** Scatter plot comparing CC vs. RMSE for each measurement and an estimation technique for daily precipitation accumulations from 13 to 16 September 2024 against data from manual rain gauges (GAU Manual) as reference.



**Figure 9.** Scatter plot comparing CC vs. RMSE for each measurement and estimation technique for hourly precipitation accumulations from 13 to 16 September 2024, against the RainGRS estimates (GRS) as reference.

tively. The raw radar data (RAD) also correlate well with the reference, achieving a CC of 0.90; however, the discrepancies between values are larger, resulting in an RMSE of 1.1 mm. It is important to note that the GRS products depend on all three data fields.

Among the other data not involved in multi-source Rain-GRS combination, relatively high reliability was preserved by the CML field, with the best correlation coefficient (CC=0.67), but Bias is significant (Bias=-0.4), even though the RMSE is not relatively high (RMSE= $1.1\,\mathrm{mm}$ ). Model simulations ERA5 and WRF do not correlate well with the reference (CC=0.50 and 0.37, respectively), and the discrepancy in value is large (RMSE of 1.3 and 1.7 mm, respectively).

IMERG analyses proved to be the most reliable satellite-based products compared in this work. By incorporating multiple precipitation data sources, which takes several months, a correlation with reference (CC=0.53) is better than both model simulations but worse than that obtained by rain gauge, radar measurements, and even CMLs. The statistics for the other satellite-based estimates (SAT, H61B, and PDIR-Now) turned out to be much worse: CC < 0.26 and RMSE > 1.7 mm; moreover, they drastically underestimate rainfall (their negative Bias is more than 0.35 mm).

# 4.4 Verification of extreme daily and hourly precipitation accumulations

For effective flood protection, it is important to have accurate values of very high precipitation. In order to assess the reliability of the measurements and estimations of extreme accumulations, verification was conducted by introducing a threshold on the minimum reference precipitation value.

The results of the statistical analysis based on daily accumulations from manual rain gauge measurements (GAU Manual) for days with recorded rainfall of 50 mm or more are presented in Table 4. The relationship between CC and RMSE values for the verified measurement techniques is shown in the graph in Fig. 10.

As expected, the results are noticeably worse when compared to those obtained without a limitation on precipitation magnitude (see Table 2). This is particularly evident in terms of Bias, which indicates an increase in underestimation. However, a negative Bias was observed for all the estimation techniques analysed, even without thresholding. This suggests a real underestimation of intense precipitation by these methods, rather than simply a result of data selection. Excellent agreement with the reference high precipitation was obtained by rain gauge observations (GAU) and estimates directly based on measurements (RAD Adj and GRS), for which CC > 0.85 and RMSE < 25 mm. The estimate based solely on radar data (RAD) correlates quite well (CC = 0.61), but the values are strongly underestimated (RMSE = 63.8 mm, bias = -58.1 mm).

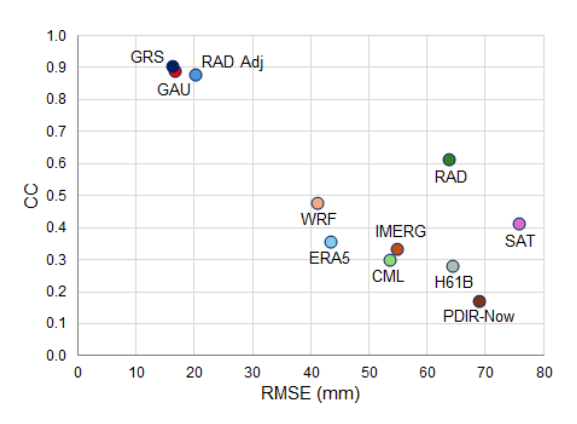


**Figure 10.** Scatter plot comparing CC vs. RMSE for each measurement and estimation technique for daily precipitation accumulations from 13 to 16 September 2024 against data from manual rain gauges (GAU Manual) as a reference, with a threshold of 50 mm.

**Table 4.** Values of statistics for daily precipitation accumulations from 13 to 16 September 2024 against data from manual rain gauges (GAU Manual) as a reference, with a threshold for daily precipitation of 50 mm.

Measurement/ estimation technique	Mean (mm)	CC (-)	RMSE (mm)	RRSE (-)	Bias (mm)				
Reference data									
GAU Manual	84.38	-	-	-	-				
Available in rea	l time								
GAU	76.90	0.889	16.66	0.53	-7.49				
RAD	26.30	0.614	63.76	2.03	-58.08				
RAD Adj	70.81	0.880	20.18	0.64	-13.57				
SAT	14.43	0.413	75.63	2.40	-69.95				
H61B	28.42	0.283	64.20	2.04	-55.96				
CML	42.06	0.301	53.58	1.70	-42.32				
GRS	75.89	0.904	16.09	0.51	-8.49				
Available offline									
IMERG	39.75	0.336	54.82	1.74	-44.64				
PDIR-Now	23.49	0.170	68.81	2.19	-60.89				
ERA5	54.33	0.357	43.28	1.37	-30.05				
WRF	56.51	0.479	41.14	1.31	-27.87				

All satellite-based data are inconsistent with the benchmark, as indicated by the low correlation (CC < 0.42) and significant differences in precipitation values (RMSE > 50 mm). The IMERG product also has low reliability, although it outperformed the other satellite-derived estimates in previous verifications.

The result of the verification of the CML estimates is quite surprising compared to the earlier ones: they have a relatively low correlation (CC = 0.30) and a rather high RMSE (53.6 mm). This can be explained by the non-uniform distribution of transmitting and receiving stations: in the moun-

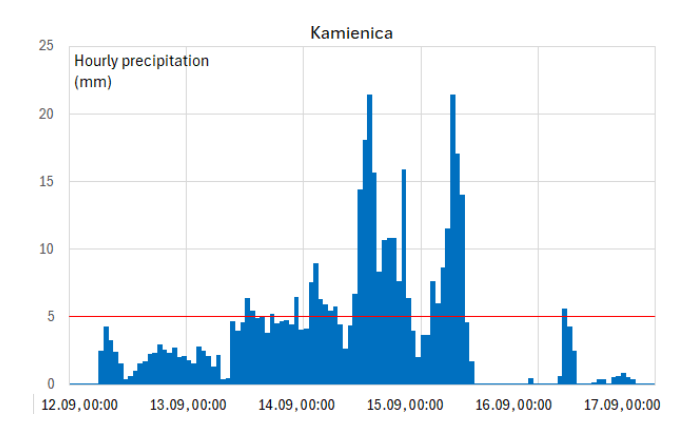


**Figure 11.** Hyetogram of 1 h RainGRS estimates (GRS) at the location of the Kamienica rain gauge station. The red line indicates the 5 mm threshold of hourly precipitation accumulations.

tains – where the highest precipitation was recorded – their network is much sparser compared to other areas (the opposite in the case of rain gauge networks).

The ERA5 and WRF model simulations have similar errors on precipitation values (RMSE  $\sim$  42 mm), but the correlation is a bit better for the WRF model (CC = 0.48), which may be due to the much higher spatial resolution of this model. In previous verifications (Table 2), models achieved comparable results regarding both CC and RMSE. The models still outperform satellite-based estimates.

A similar analysis was conducted, but the reliability of measurements and precipitation estimates for high precipitation were verified using hourly accumulations instead of daily accumulations. The results are depicted in Table 5 and in the graph in Fig. 12. In this case, the reference dataset consists of RainGRS estimates (GRS), applying a threshold for hourly precipitation accumulation of 5 mm, with the assumption that there must be at least 200 pixels (out of a total of 44 218 pixels) fulfilling this requirement in a given time step. Thresholds of 5 mm for hourly accumulations and 200 pixels for the area where such precipitation occurred (approximately 0.5 % of the entire basin) were introduced to exclude data with low precipitation from the statistics. Figure 11 shows, as an example, the multi-source GRS hyetogram at the Kamienica manual rain gauge location, which recorded the highest 4 d precipitation accumulation of all the stations in the flood area.

In this verification, the statistical results are significantly worse than in Table 3, as correctly reproducing extremely high hourly precipitation accumulations is challenging. Only GAU, RAD, and RAD Adj measurements provide relatively reliable results regarding correlation with GRS (CC > 0.50). As in the previous analyses, the estimate based solely on RAD data gives a significant underestimation of rainfall (RMSE =  $4.3 \, \text{mm}$ , bias =  $-4.1 \, \text{mm}$ ), while for the fields based on rain gauge data, these errors are much lower: the RMSE for GAU and RAD Adj is 2.5 and 0.8 mm, respec-

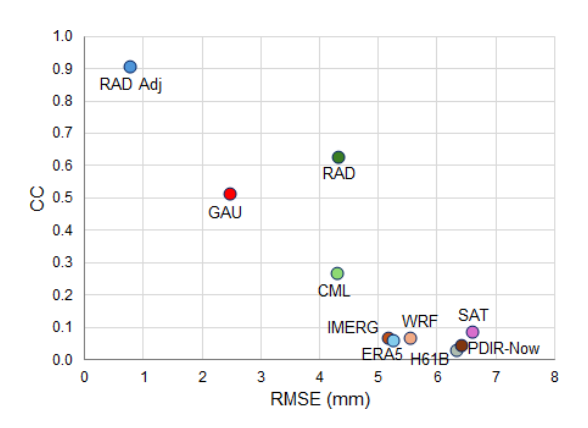


**Figure 12.** Scatter plot comparing CC vs. RMSE for each measurement and estimation technique for hourly precipitation accumulations from 13 to 16 September 2024 against the RainGRS estimates (GRS) as a reference, with a threshold of 5 mm.

**Table 5.** Values of statistics for hourly precipitation accumulations from 13 to 16 September 2024 against the RainGRS estimates (GRS) as a reference, with a threshold for hourly precipitation of 5 mm.

Measurement/ estimation technique	Mean (mm)	CC (-)	RMSE (mm)	RRSE (-)	Bias (mm)
Reference data					
GRS	7.03	-	-	-	-
Available in real time					
GAU (dependent)	5.29	0.515	2.46	1.63	-1.75
RAD (dependent)	2.96	0.630	4.32	2.92	-4.08
RAD Adj (dependent)	7.02	0.907	0.76	0.57	-0.01
SAT (dependent)	0.85	0.089	6.60	4.68	-6.19
H61B	1.21	0.029	6.33	4.41	-5.83
CML	3.37	0.269	4.28	2.96	-3.66
Available offline					
IMERG	2.60	0.069	5.16	3.42	-4.44
PDIR-Now	1.06	0.046	6.40	4.43	-5.97
ERA5	2.27	0.062	5.24	3.57	-4.77
WRF	2.38	0.069	5.54	3.84	-4.66

tively. However, it is important to note that the GRS reference depends on all estimates using rain gauge or radar data.

Among the datasets not involved in multi-source RainGRS estimation, none of the correlations exceed CC = 0.1 except for the CML estimate (CC = 0.27). The values of RMSE and Bias are also high for them (RMSE > 5 mm, Bias between -4 and -6).

The conclusion from this analysis is that the estimation of extremely high precipitation fields with very high spatial (1 km) and temporal (1 h) resolution is mainly based on weather radar observations, but these must first be adjusted to the rain gauge data. Rain gauges can also produce reliable es-

timates but under the condition that a sufficiently dense network of such gauges is available.

#### 4.5 Analyses for selected stations

Four stations with manual rain gauges (GAU Manual) were selected to check the consistency of the precipitation estimated by different techniques and models concerning particular locations for 4 d with the highest values during the flood. They are located in different regions of the basin, where intense rainfall was observed (Fig. 4), moving from west to east of the Sudety Mountains:

- Szklarska Poreba in the Karkonosze Mountains,
- Kamienica in the Śnieżnik Mountains near the Kłodzko Valley (the highest daily as well as 4 d precipitation was observed there during this flood),
- Głuchołazy, situated in the foothills of the Opawskie Mountains,
- Gołkowice, located in the Ostrava Valley.

Table A1 presents accumulations for all verified measurements and estimates for individual days and the 4 d totals in these locations. In Szklarska Poręba and Kamienica, telemetric rain gauges (GAU) measured daily accumulations very close to the reference rainfall (GAU Manual), while the other two locations underestimated by about 10 %–20 %. The daily distribution of RAD values indicates good temporal alignment with the GAU Manual, but a significant underestimation of rainfall is evident. Adjustment of the radar-based estimates to rain gauge measurements resulted in a significant increase in RAD Adj values, but they are still lower than the GAU Manual at all locations except Gołkowice. GRS precipitation accumulations for three stations (Szklarska Poreba, Kamienica, and Głuchołazy) are similar to GAU, i.e. also underestimated in relation to the reference by about 10 %–20 %. At the Gołkowice location, where there is no telemetric rain gauge and the GAU values are derived from interpolation, the GRS estimates are very close to the RAD Adj values and overestimate the benchmark.

Estimates based on CML data are significantly lower than the reference, except Szklarska Poreba, where the density of the microwave link network is relatively high. This underestimation in the other stations is probably due to the lack of links near them, so values are derived from the interpolation of slightly more distant links, usually located at lower altitudes, which record less precipitation.

The variability of all satellite-based precipitation in the analysed days does not correspond well with the daily distribution of the reference. Accumulations are much lower in comparison to values measured by manual rain gauges. The IMERG reanalyses slightly outperform the others, which is similar to previous investigations.

Mesoscale model simulations are also underestimated, although the WRF model does so to a lesser extent. They better reflect the temporal distribution of daily precipitation accumulations and their magnitudes than satellite data.

The cumulative precipitation curves obtained from 1 h accumulations for the same four stations are shown in Fig. 13. The GAU Manual data generated with a daily step were not included, and in consequence, the GRS estimates (see Sect. 4.3) were taken as a reference to assess the consistency of temporal distributions of verified precipitation. It can be seen from analyses of the curves for all four stations that the estimates on which the GRS data depend, i.e. those based on rain gauge and radar measurements, are similar to each other, although the differences between the reference and the values derived solely from radar observations are very large. In terms of the independent data, the curves for CML and WRF reflect the temporal distribution of precipitation relatively correctly. In contrast, all satellite-based estimates are highly inconsistent with the reference, taking into account precipitation variability in time, and among them, the IMERG reanalyses indicate the best temporal alignment, as in previous investigations.

# 4.6 Overall assessment of the various rainfall measurement techniques

The evaluation of the results obtained in this study is mainly based on the numerical values summarised in Tables 2–5, where the reliability statistics of the individual measurements and estimations are shown. The analyses were conducted with daily accumulations from the GAU Manual (Tables 2 and 4) and 1 h RainGRS estimates as references (Tables 3 and 5). It should be noted that the latter depends, to differing degrees, on data involved in multi-source combination GAU, RAD, and RAD Adj, and, to a lesser extent, on SAT product. Nevertheless, the proportions between the statistics' values are similar using both references. This leads to the conclusion that this dependence has little influence on the final outcomes; however, the following overall assessment does not include findings from the analysis of the consistency of individual data with the reference dependent on them.

# 4.6.1 Rain gauge data

Spatially interpolated telemetric precipitation data (GAU) proved to be very similar to measurements from manual rain gauges (GAU Manual), but they generally provide slightly lower values (Tables 2 and 4). The accuracy of the rain gauge observations also remains high if only heavy precipitation is considered, which is confirmed by the statistics calculated after introducing an appropriate threshold on the daily accumulations, as can be seen from a comparison of Tables 2 and 4.

Notably, 76 out of 158 telemetric rain gauges are in the same locations as the manual ones in the flood area. This sig-

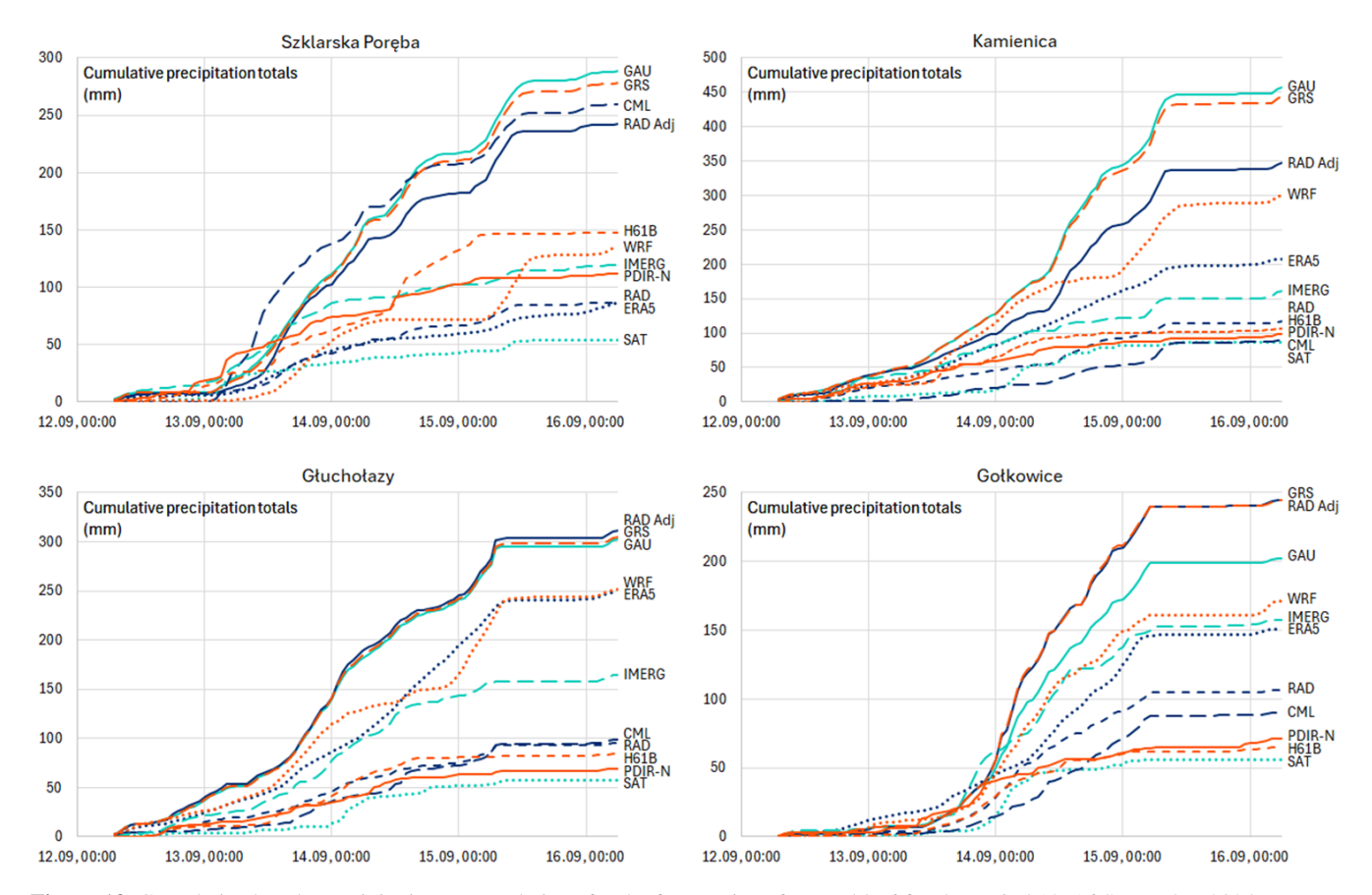


Figure 13. Cumulative hourly precipitation accumulations for the four stations from Table 6 for the period 13–16 September 2024.

nificantly impacts the reliability statistics calculated for the GAU data as, in the case of an interpolated field, estimated values strongly depend on the distance to the nearest station.

### 4.6.2 Weather-radar-based data

Weather radars reflect the spatial and temporal distributions of the precipitation field very well, as evidenced by the very high CC correlation coefficients with the reference presented in all tables, especially Tables 2 and 4, where the benchmark data are independent of the radar measurements.

Raw radar estimates RAD produced significantly underestimated precipitation values, as indicated, for example, by the very large Bias values (Tables 2 and 4). Adjusting with telemetric rain gauge data considerably improves this and makes the corrected radar-based precipitation field (RAD Adj) very close in precipitation values to both the GAU Manual and GRS reference estimates.

Analysing only high precipitation, i.e. after introducing an appropriate threshold on the amount of daily precipitation accumulation, the results were analogous to the analysis without applying a threshold (Table 4 vs. Table 2). This confirms the high reliability of the radar measurements also in the case of heavy precipitation; however, the data without adjustment are subject to a large Bias.

# 4.6.3 Satellite-based data

The satellite-based real-time SAT and H61B fields, based on the products from the EUMETSAT NWC SAF and H SAF programmes, respectively, turned out to be practically useless for the precipitation estimation in the case study analysed here. They correlate poorly with reference and significantly underestimate values of precipitation accumulation (Tables 2 and 3). The primary reason is that they are mainly based on data from geostationary satellites – the only kind that can be used directly for real-time measurements at a high temporal resolution. Among the more advanced satellite-based precipitation products available (only offline analysed in this work), it can be stated that the PDIR-Now estimates are definitely wrong. The IMERG reanalysis proved significantly better, although its reliability is also not high.

If the highest daily accumulations are considered by limiting them to values above the threshold of 50 mm d<sup>-1</sup>, only SAT precipitation based on NWC SAF products shows some agreement with the reference, although it is weak (Table 4). The correlations of all satellite estimates decrease dramatically for extreme 1 h accumulations (Table 5).

#### 4.6.4 Multi-source estimates

The multi-source GRS estimates are generated by the Rain-GRS system for the merging GAU, RAD Adj, and SAT precipitation measurements. The analyses carried out in this study showed that these fields, among all the verified data available in real time, are in the best agreement with independent reference observations from manual rain gauges (GAU Manual) (Tables 2 and 4). The metrics are slightly better than those for spatially interpolated rain gauges, but the multisource estimates significantly outperform the others. This results from the combination that utilises the individual inputs' positive features (see Sects. 1.2.2 and 3.2.5).

#### 4.6.5 CML-based estimates

CML-based estimates correlate relatively well with daily and hourly accumulation benchmarks, but relatively high errors relate to differences between verified and reference values: RMSE and Bias. Data estimated from the measurements of signal attenuation from commercial microwave links in precipitation are clearly better than satellite-derived fields, even those available offline, but they are worse than estimates based on rain gauge and radar information. Their reliability is similar to mesoscale model simulations in terms of daily data; however, for hourly accumulations, the CML-based estimates outperform them (Tables 2 and 3). This suggests better representativeness in the temporal distribution of precipitation.

These relatively good statistics for CML-based data are probably because the network of links is very dense relative to the rain gauge network, which partly compensates for their much higher uncertainty. However, there are considerably fewer links in the highest less urbanised mountainous areas, where precipitation is usually more intense and the detection of extreme precipitation is consequently subject to more significant errors (Tables 4 and 5).

# 4.6.6 NWP-based reanalyses

The NWP simulations have higher reliability than satellite data but clearly lower than radar and rain gauge measurements. Their metrics are similar when analysing daily accumulations (Table 2), whereas for hourly ones, they turned out worse in comparison with the CML-based data (Table 3).

The results obtained by the ERA5 and WRF models are ambiguous. In terms of daily accumulation investigations, the reliability of both models is comparable. When analysing 1 h data (Table 3), the ERA5 reanalyses proved to be better, although their CC is not high, which indicates a more correct alignment of the precipitation variability in time. In turn, the WRF model performed better if the highest daily accumulations were considered, i.e. only above 50 mm d<sup>-1</sup> (Table 4). This is probably due to the significantly higher (around 20 times) spatial resolution of the WRF model com-

pared to ERA5, which increases their usefulness for detailed analyses of precipitation more variable in space. When it comes to extreme hourly precipitation, i.e. with a threshold for precipitation above 5 mm, none of the mesoscale models are reliable: correlations with the GRS field do not exceed CC = 0.10 for both (Table 5).

# 5 Conclusions

In this work, detailed analyses were carried out of the reliability of different precipitation measurements and estimations during a large flood in Poland in 2024, caused by extremely high widespread precipitation in an orographically diversified basin.

Their reliability was evaluated using precipitation field or point observations assumed to be closest to reality (ground truth). As a reference, data from manual rain gauges (GAU Manual) were chosen as they are considered to be the most accurate, but they are point-wise and have the limitation of a temporal resolution of 1 d. In order to test the usefulness of data with a higher 1 h temporal resolution, RainGRS estimates (GRS) were used as a benchmark. In addition, similar analyses were conducted, but only the most intense precipitation was considered by applying appropriate thresholds (over  $50 \, \mathrm{mm} \, \mathrm{d}^{-1}$  and  $5 \, \mathrm{mm} \, \mathrm{h}^{-1}$ ).

Comparing the various precipitation fields available in real time, the data based on telemetric rain gauge measurements (GAU) and weather radar observations after adjustment with rain gauge data (RAD Adj), as well as the multi-source estimates (GRS) derived from a combination of these two types of data supplemented with satellite information, are definitely most reliable. It can be concluded that during intense precipitation events triggering floods, even in mountainous areas, rain gauge and radar measurements are sufficient for accurate real-time monitoring of the precipitation field with high spatial and temporal resolution, even though IMGW's measurement networks are not very dense compared to those of other European countries.

Among the other precipitation data sources, CML-based estimates proved to be the most accurate. This is surprising as they are based on non-standard measurements, but their strength is the very high number of microwave links available. However, these data indicate significant underestimation of precipitation, highlighting the need for more sophisticated quality control and bias correction.

Reliability analyses of satellite data show that they are generally of little usefulness, apart from the IMERG estimates. Their relatively good agreement with the reference is due to incorporating a higher number of different types of satellite measurements, mainly microwave. However, this involves long waiting times for the final estimates, which rather excludes them from operational applications, although they can be helpful in reanalyses.

The research showed the limited suitability of mesoscale model simulations for analyses with high temporal and spatial resolution. At the same time, their reliability is sufficient for use when such a requirement is not necessary. Consequently, they are not particularly useful for analyses of very intense and spatially variable precipitation.

# Appendix A

**Table A1.** Comparison of daily and 4 d precipitation accumulations for four selected stations at locations of manual rain gauges (Szklarska Poręba, Kamienica, Głuchołazy, Gołkowice).

Measurement/	Station: Szklarska Poręba					Station: Kamienica				
estimation technique	13 Sep	14 Sep	15 Sep	16 Sep	4 d	13 Sep	14 Sep	15 Sep	16 Sep	4 d
Reference data										
GAU Manual	20.0	123.8	84.9	63.5	292.2	51.1	114.2	254.5	52.7	472.5
Available in rea	l time									
GAU	21.72	131.15	85.11	50.47	288.45	49.60	120.2	236.82	51.39	458.01
RAD	10.27	40.51	22.94	12.71	86.43	26.09	27.06	52.08	12.29	117.52
RAD Adj	13.57	120.53	69.03	38.96	242.09	48.08	80.08	179.46	40.12	347.74
SAT	23.22	14.51	7.24	9.30	54.27	9.19	41.90	30.59	5.16	86.84
H61B	24.63	37.53	78.68	0.42	141.26	23.90	57.44	29.77	6.28	117.38
CML	29.89	136.66	56.68	36.03	259.26	2.50	22.38	40.24	24.77	89.89
GRS	20.06	130.96	79.72	47.38	278.12	50.61	118.06	227.15	48.71	444.53
Available offline	e									
IMERG	31.85	58.41	15.22	14.27	119.75	40.54	61.81	39.81	18.72	160.88
PDIR-Now	42.00	35.00	31.00	4.00	112.00	29.00	40.00	19.00	11.00	99.00
ERA5	9.18	41.43	12.75	23.17	86.53	33.51	67.34	82.21	24.69	207.75
WRF	1.81	65.93	7.43	59.28	134.45	33.69	118.82	95.69	52.53	300.73
Measurement/		Stati	on: Głucho	ołazy		Station: Gołkowice				
estimation technique	13 Sep	14 Sep	15 Sep	16 Sep	4 d	13 Sep	14 Sep	15 Sep	16 Sep	4 d
Reference data										
GAU Manual	56.0	158.2	124.3	23.0	361.5	9.7	96.2	118.2	3.8	227.9
Available in rea	l time									
GAU	51.19	131.35	93.33	26.81	302.68	7.62	90.22	101.27	3.29	202.40
RAD	19.55	39.66	26.95	9.28	95.44	3.64	49.18	51.86	2.05	106.73
RAD Adj	53.86	135.36	93.61	28.37	311.20	7.29	111.65	120.89	4.50	244.33
SAT	3.84	32.80	15.95	4.97	57.56	1.31	39.89	14.55	0.33	56.08
H61B	10.90	48.14	26.09	3.64	88.77	3.63	52.41	22.20	2.67	80.90
CML	8.95	34.09	43.32	11.76	98.12	2.50	22.14	63.43	2.11	90.18
GRS	51.82	133.06	93.40	26.77	305.05	7.96	113.61	118.33	4.26	244.16
Available offline	e									
IMERG	26.13	74.61	54.68	9.20	164.62	7.77	67.48	77.85	4.48	157.58
PDIR-Now	15.00	28.00	21.00	5.00	69.00	6.00	39.00	20.00	6.00	71.00
			122.77	21.64	248.70	17.09	38.64	90.38	4.66	150.76
ERA5	36.01	68.28	144.77	41.U <del>4</del>	4 <del>4</del> 0.70	17.02	30.U <del>1</del>	20.20	7.00	

Code availability. The data processing codes are protected by the economic property rights of the software and are not available for distribution. The codes used for processing follow the methodologies and equations described herein.

Data availability. Out of the data used in this paper, the following are publicly available:

- Rain gauge, weather radar, RainGRS, satellite (SAT and H61B) data of IMGW: https://danepubliczne.imgw.pl/pl/ datastore (last access: 14 October 2025), tab: "Dane archiwalne",
- IMERG (https://doi.org/10.5067/GPM/IMERG/3B-HH/07, NASA, 2025),
- PDIR-Now: https://persiann.eng.uci.edu/CHRSdata/ PDIRNow/PDIRNow1hourly/ (last access: 14 October 2025),
- ERA5 data (https://cds.climate.copernicus.eu/datasets/ reanalysis-era5-single-levels, ECMWF, 2025).

Other data used in this paper are available upon request, provided they are not restricted by the producer.

Author contributions. AJ, JS, and KO developed the concept for the paper. MF carried out the simulations with the WRF model. MS developed the software and carried out the processing of various types of data. KO and AK developed the software and carried out the statistical calculations. AJ, JS, KO, MS, and AK conducted an analysis of the results. JS, AJ, and KO wrote the text of the paper. MS, AK, RP, and MF verified the text. JS and AJ created the figures.

Competing interests. The contact author has declared that none of the authors has any competing interests.

Disclaimer. Publisher's note: Copernicus Publications remains neutral with regard to jurisdictional claims made in the text, published maps, institutional affiliations, or any other geographical representation in this paper. While Copernicus Publications makes every effort to include appropriate place names, the final responsibility lies with the authors. Views expressed in the text are those of the authors and do not necessarily reflect the views of the publisher.

Acknowledgements. All simulations using the WRF model were performed at the Academic Computer Centre in Gdansk (CI TASK).

*Review statement.* This paper was edited by Serena Ceola and reviewed by Nicolas Velasquez and two anonymous referees.

#### References

- Afzali Gorooh, V., Shearer, E. J., Nguyen, P., Hsu, K., Sorooshian, S., Cannon, F., and Ralph, M.: Performance of new near-real-time PERSIANN product (PDIR-Now) for Atmospheric River Events over the Russian River Basin, California, J. Hydrometeorol., 23, 1899–1911, https://doi.org/10.1175/JHM-D-22-0066.1, 2022.
- Berthomier, L. and Perier, L.: Espresso: A global deep learning model to estimate precipitation from satellite observations, Meteorology, 2, 421–444, https://doi.org/10.3390/meteorology2040025, 2023.
- Bissolli, P., Friedrich, K., Rapp, J., and Ziese, M.: Flooding in eastern central Europe in May 2010 reasons, evolution and climatological assessment, Weather, 66, 147–153, https://doi.org/10.1002/wea.759, 2011.
- Bližňák, V., Kašpar, M., Müller, M., and Zacharov, P.: Subdaily temporal reconstruction of extreme precipitation events using NWP model simulations, Atmos. Res., 224, 65–80, https://doi.org/10.1016/j.atmosres.2019.03.019, 2019.
- Bližňák, V., Pokorná, L., and Rulfová, Z.: Assessment of the capability of modern reanalyses to simulate precipitation in warm months using adjusted radar precipitation, J. Hydrol.: Reg. Stu., 42, 101121, https://doi.org/10.1016/j.ejrh.2022.101121, 2022.
- Bogerd, L., Overeem, A., Leijnse, H., and Uijlenhoet, R.: A comprehensive five-year evaluation of IMERG Late Run precipitation estimates over the Netherlands, J. Hydrometeorol., 22, 1855–1868, https://doi.org/10.1175/JHM-D-21-0002.1, 2021.
- Bojinski, S., Blaauboer, D., Calbet, X., de Coning, E., Debie, F., Montmerle, T., Nietosvaara, V., Norman, K., Bañón Peregrín, L., Schmid, F., Strelec Mahović, N., and Wapler, K.: Towards nowcasting in Europe in 2030, Meteorol. Appl., 30, e2124, https://doi.org/10.1002/met.2124, 2023.
- CHRS: Data portal, https://chrsdata.eng.uci.edu/ (last access: 29 July 2025), 2025.
- DWD: ICON (Icosahedral Nonhydrostatic) Model, https://www.dwd.de/EN/research/weatherforecasting/num\_modelling/01\_num\_weather\_prediction\_modells/icon\_description.html (last access: 29 July 2025), 2025.
- ECMWF: ERA5 hourly data on single levels from 1940 to present, ECMWF [data set], https://cds.climate.copernicus.eu/datasets/reanalysis-era5-single-levels (last access: 29 July 2025), 2025.
- Ensor, L. A. and Robeson, S. M.: Statistical characteristics of daily precipitation: comparisons of gridded and point datasets, J. Appl. Meteorol. Clim., 47, 2468–2476, https://doi.org/10.1175/2008JAMC1757.1, 2008.
- EUMETSAT: H SAF: Algorithm Theoretical Baseline Document (ATBD) for product H61 P-AC-SEVIRI-PMW and H90 P-AC-SEVIRI\_E. Accumulated precipitation at ground by blended MW and IR, https://hsaf.meteoam.it/CaseStudy/GetDocumentUserDocument? fileName=saf\_hsaf\_atbd-61b-90b\_1\_0.pdf&tipo=ATBD (last access: 17 April 2025), 2020.
- EUMETSAT: NWC SAF: Algorithm Theoretical Ba-Document for the Precipitation Product Prosis NWC/GEO, cessors the https://www.nwcsaf.org/ Downloads/GEO/2021/Documents/Scientific\_Docs/ NWC-CDOP3-GEO-AEMET-SCI-ATBD-Precipitation\_ v1.0.1.pdf (last access: 17 April 2025), 2021.

- Fischer, J., Groenemeijer, P., Holzer, A., Feldmann, M., Schröer, K., Battaglioli, F., Schielicke, L., Púčik, T., Antonescu, B., Gatzen, C., and TIM Partners: Invited perspectives: Thunderstorm intensification from mountains to plains, Nat. Hazards Earth Syst. Sci., 25, 2629–2656, https://doi.org/10.5194/nhess-25-2629-2025, 2025.
- Garcia-Marti, I., Overeem, A., Noteboom, J. W., de Vos, L., de Haij, M., and Whan, K.: From proof-of-concept to proof-of-value: Approaching third-party data to operational workflows of national meteorological services. Int. J. Climatol., 43, 275–292, https://doi.org/10.1002/joc.7757, 2023.
- Goudenhoofdt, E. and Delobbe, L.: Evaluation of radar-gauge merging methods for quantitative precipitation estimates, Hydrol. Earth Syst. Sci., 13, 195–203, https://doi.org/10.5194/hess-13-195-2009, 2009.
- Graf, M., Chwala, C., Polz, J., and Kunstmann, H.: Rainfall estimation from a German-wide commercial microwave link network: optimised processing and validation for 1 year of data, Hydrol. Earth Syst. Sci., 24, 2931–2950, https://doi.org/10.5194/hess-24-2931-2020, 2020.
- Graf, M., Wagner, A., Polz, J., Lliso, L., Lahuerta, J. A., Kunstmann, H., and Chwala, C.: Improved rain event detection in commercial microwave link time series via combination with MSG SEVIRI data, Atmos. Meas. Tech., 17, 2165–2182, https://doi.org/10.5194/amt-17-2165-2024, 2024.
- Henn, B., Newman, A. J., Livneh, B., Daly, C., and Lundquist, J. D.: An assessment of differences in gridded precipitation datasets in complex terrain, J. Hydrol., 556, 1205–1219, https://doi.org/10.1016/j.jhydrol.2017.03.008, 2018.
- Herrera, S., Kotlarski, S., Soares, P. M. M., Cardoso, R. M., Jaczewski, A., Gutiérrez, J. M., and Maraun, D.: Uncertainty in gridded precipitation products: Influence of station density, interpolation method and grid resolution, Int.J. Climatol., 39, 3717–3729, https://doi.org/10.1002/joc.5878, 2019.
- Hersbach, H., Bell, B., Berrisford, P., Hirahara, S., Horányi, A., Muñoz-Sabater, J., Nicolas, J., Peubey, C., Radu, R., Schepers, D., Simmons, A., Soci, C., Abdalla, S., Abellan, X., Balsamo, G., Bechtold, P., Biavati, G., Bidlot, J., Bonavita, M., De Chiara, G., Dahlgren, P., Dee, D., Diamantakis, M., Dragani, R., Flemming, J., Forbes, R., Fuentes, M., Geer, A., Haimberger, L., Healy, S., Hogan, R. J., Hólm, E., Janisková, M., Keeley, S., Laloyaux, P., Lopez, P., Lupu, C., Radnoti, G., de Rosnay, P., Rozum, I., Vamborg, F., Villaume, S., and Thépaut, J.-N.: The ERA5 global reanalysis, Q. J. Roy. Meteorol. Soc., 146, 1999–2049, https://doi.org/10.1002/qj.3803, 2020.
- Hoffmann, M., Schwartengräber, R., Wessolek, W., and Peters, A.: Comparison of simple rain gauge measurements with precision lysimeter data, Atmos. Res., 174–175, 120–123, https://doi.org/10.1016/j.atmosres.2016.01.016, 2016.
- Hohmann, C., Kirchengast, G., O, S., Rieger, W., and Foelsche, U.: Small catchment runoff sensitivity to station density and spatial interpolation: hydrological modeling of heavy rainfall using a dense rain gauge network, Water, 13, 1381, https://doi.org/10.3390/w13101381, 2021.
- Huffman, G. J., Bolvin, D. T., Braithwaite, D., Hsu, K.-L., Joyce,
  R. J., Kidd, C., Nelkin, E. J., Sorooshian, S., Stocker, E. F.,
  Tan, J., Wolff, D. B., and Xie, P.: Integrated Multi-satellite
  Retrievals for the Global Precipitation Measurement (GPM)
  Mission (IMERG), in: vol. 1., Satellite Precipitation Measure-

- ment, Advances in Global Change Research, vol. 67, edited by: Levizzani, V., Kidd, C., Kirschbaum, D. B., Kummerow, C. D., Nakamura, K., and Turk, F. J., Springer, Cham, 343–353, https://doi.org/10.1007/978-3-030-24568-9\_19, 2020.
- Iacono, M. J., Delamere, J. S., Mlawer, E. J., Shephard, M. W., Clough, S. A., and Collins, W. D.: Radiative forcing by long-lived greenhouse gases: Calculations with the AER radiative transfer models, J. Geophys. Res.-Atmos., 113, D13103, https://doi.org/10.1029/2008JD009944, 2008.
- Jarvis, P. G.: The interpretation of the variations in leaf water potential and stomatal conductance found in canopies in the field, Philos. T. Roy. Soc. B, 273, 593–610, https://doi.org/10.1098/rstb.1976.0035, 1976.
- Jiang, Q., Li, W., Wen, J., Fan, Z., Chen, Y., Scaioni, M., and Wang, J.: Evaluation of satellite-based products for extreme rainfall estimations in the eastern coastal areas of China, J. Integrat. Environ. Sci., 16, 191–207, https://doi.org/10.1080/1943815X.2019.1707233, 2019.
- Jurczyk, A., Szturc, J., and Ośródka, K.: Quality-based compositing of weather radar QPE estimates, Meteorol. Appl., 27, e1812, https://doi.org/10.1002/met.1812, 2020a.
- Jurczyk, A., Szturc, J., Otop, I., Ośródka, K., and Struzik, P.: Quality-based combination of multi-source precipitation data, Remote Sens., 12, 1709, https://doi.org/10.3390/rs12111709, 2020b
- Jurczyk, A., Ośródka, K., Szturc, J., Pasierb, M., and Kurcz, A.: Long-term multi-source precipitation estimation with high resolution (RainGRS Clim), Atmos. Meas. Tech., 16, 4067–4079, https://doi.org/10.5194/amt-16-4067-2023, 2023.
- Kimutai, J., Vautard, R., Zachariah, M., Tolasz, R., Šustková, V., Cassou, C., Skalák, P., Clarke, B., Haslinger, K., Vahlberg, M., Singh, R., Stephens, E., Cloke, H., Raju, E., Baumgart, N., Thalheimer, L., Chojnicki, B., Otto, F., Koren, G., Philip, S., Kew, S., Haro, P., Vibert, J., and Von Weissenberg, A.: Climate change and high exposure increased costs and disruption to lives and livelihoods from flooding associated with exceptionally heavy rainfall in Central Europe, Report, IMPERIAL, p. 36, https://doi.org/10.25561/114694, 2024.
- Kundzewicz, Z. W.: Adapting flood preparedness tools to changing flood risk conditions: the situation in Poland, Oceanologia, 56, 385–407, https://doi.org/10.5697/oc.56-2.385, 2014.
- Kundzewicz, Z. W., Januchta-Szostak, A., Nachlik, E., Pińskwar, I., and Zaleski, J.: Challenges for flood risk reduction in Poland's changing climate, Water, 15, 2912, https://doi.org/10.3390/w15162912, 2023.
- Ligenza, P., Tokarczyk, T., and Adynkiewicz-Piragas, M. (Eds.): Przebieg i skutki wybranych powodzi w dorzeczu Odry od XIX wieku do czasów współczesnych (The course and impacts of selected floods in the Oder river basin from the XIXth century to the present day), Instytut Meteorologii i Gospodarki Wodnej – Państwowy Instytut Badawczy, Warszawa, 132 pp., ISBN 978-83-64979-45-3, 2021.
- Loritz, R., Hrachowitz, M., Neuper, M., and Zehe, E.: The role and value of distributed precipitation data in hydrological models, Hydrol. Earth Syst. Sci., 25, 147–167, https://doi.org/10.5194/hess-25-147-2021, 2021.
- Mahmoud, M. T., Mohammed, S. A., Hamouda, M. A., Dal Maso, M., and Mohamed, M. M.: Performance of the IMERG precip-

- itation products over high-latitudes region of Finland, Remote Sens., 13, 2073, https://doi.org/10.3390/rs13112073, 2021.
- Mai, X., Zhong, H., and Li, L.: Combination of XG-Boost and PPLK method for improving the precipitation nowcasting, MATEC Web Conf., 355, 03039, https://doi.org/10.1051/matecconf/202235503039, 2022.
- Méri, L., Gaál, L., Bartok, J., Gažák, M., Gera, M., Jurašek, M., and Kelemen, M.: Improved radar composites and enhanced value of meteorological radar data using different quality indices, Sustainability, 13, 5285, https://doi.org/10.3390/su13095285, 2021.
- Merino, A., García-Ortega, E., Navarro, A., Fernández-González, S., Tapiador, F. J., and Sánchez, J. L.: Evaluation of gridded rain-gauge-based precipitation datasets: Impact of station density, spatial resolution, altitude gradient and climate, Int. J. Climatol., 41, 3027–3043, https://doi.org/10.1002/joc.7003, 2021.
- Mikołajewski, K., Stach, A., Ruman, M., Kosek, K., Kundzewicz, Z. W., and Licznar, P.: Heavy rainfalls in Poland and their hyetographs, Ambio, 54, 86–104, hhttps://doi.org/10.1007/s13280-024-02069-6, 2025.
- Militino, A. F., Ugarte, M. D., and Pérez-Goya, U.: Improving the quality of satellite imagery based on ground-truth data from rain gauge stations, Remote Sens., 10, 398, https://doi.org/10.3390/rs10030398, 2018.
- Mudelsee, M., Börngen, M., Tetzlaff, G., and Grünewald, U.: Extreme floods in central Europe over the past 500 years: Role of cyclone pathway "Zugstrasse Vb", J. Geophys. Res., 109, D23101, https://doi.org/10.1029/2004JD005034, 2004.
- Nakanishi, M. and Niino, H.: An improved Mellor–Yamada level-3 model: its numerical stability and application to a regional prediction of advection fog, Bound.-Lay. Meteorol., 119, 397–407, https://doi.org/10.1007/s10546-005-9030-8, 2006.
- Nakanishi, M. and Niino, H.: Development of an improved turbulence closure model for the atmospheric boundary layer, J. Meteorol. Soc. Jpn. Ser. II, 87, 895–912, https://doi.org/10.2151/jmsj.87.895, 2009.
- NASA: GPM IMERG Final Precipitation L3 Half Hourly 0.1 degree × 0.1 degree V07 (GPM\_3IMERGHH), NASA [data set], https://doi.org/10.5067/GPM/IMERG/3B-HH/07 (last access: 29 July 2025), 2025.
- Navarro, A., García-Ortega, E., Merino, A., Sánchez, J. L., and Tapiador, F. J.: Orographic biases in IMERG precipitation estimates in the Ebro River basin (Spain): The effects of rain gauge density and altitude, Atmos. Res., 244, 105068, https://doi.org/10.1016/j.atmosres.2020.105068, 2020.
- NCAR: Weather Research and Forecasting model WRF, https://ncar.ucar.edu/what-we-offer/models/weather-research-and-forecasting-model-wrf (last access: 29 July 2025), 2025.
- Nguyen, P., Ombadi, M., Gorooh, V. A., Shearer, E. J., Sadeghi, M., Sorooshian, S., Hsu, K., Bolvin, D., and Ralph, M. F.: PER-SIANN Dynamic Infrared–Rain Rate (PDIR-Now): A near-real-time, quasi-global satellite precipitation dataset, J. Hydrometeo-rol., 21, 2893–2906, https://doi.org/10.1175/JHM-D-20-0177.1, 2020a.
- Nguyen, P., Shearer, E. J., Ombadi, M., Gorooh, V. A., Hsu, K., Sorooshian, S., Logan, W. S., and Ralph, M.: PERSIANN Dynamic Infrared–Rain Rate model (PDIR) for high-resolution, real-time satellite precipitation estimation, B. Am. Meteorol.

- Soc., 101, E286–E302m, https://doi.org/10.1175/BAMS-D-19-0118.1, 2020b.
- Nielsen, J. M., van de Beek, C. Z. R., Thorndahl, S., Olsson, J., Andersen, C. B., Andersson, J. C. M., Rasmussen, M. R., and Nielsen, J. E.: Merging weather radar data and opportunistic rainfall sensor data to enhance rainfall estimates, Atmos. Res., 300, 107228, https://doi.org/10.1016/j.atmosres.2024.107228, 2024.
- Niu, G.-Y., Yang, Z.-L., Mitchell, K. E., Chen, F., Ek, M. B., Barlage, M., Kumar, A., Manning, K., Niyogi, D., Rosero, E., Tewari, M., and Xia, Y.: The community Noah land surface model with multiparameterization options (Noah-MP): 1. Model description and evaluation with local-scale measurements, J. Geophys. Res.-Atmos., 116, D12109, https://doi.org/10.1029/2010JD015139, 2011.
- Ochoa-Rodriguez, S., Wang, L.-P., Willems, P., and Onof, C.: A review of radar-rain gauge data merging methods and their potential for urban hydrological applications, Water Resour. Res., 55, 6356–6391, https://doi.org/10.1029/2018WR023332, 2019.
- Olsson, J., Horváth-Varga. L., van de Beek, R., Graf, M., Overeem, A., Szaton, M., Bares, V., Bezak, N., Chwala, C., De Michele, C., Fencl, M., Seidel, J., and Todorovic, A.: How close are opportunistic rainfall observations to providing societal benefits?, J. Hydrometeorol., https://doi.org/10.1175/JHM-D-25-0043.1, in press, 2025.
- Ośródka, K. and Szturc, J.: Improvement in algorithms for quality control of weather radar data (RADVOL-QC system), Atmos. Meas. Tech., 15, 261–277, https://doi.org/10.5194/amt-15-261-2022, 2022.
- Ośródka, K., Szturc, J., and Jurczyk, A.: Chain of data quality algorithms for 3-D single-polarisation radar reflectivity (RADVOL-QC system), Meteorol. Appl., 21, 256–270, https://doi.org/10.1002/met.1323, 2014.
- Ośródka, K., Otop, I., and Szturc, J.: Automatic quality control of telemetric rain gauge data providing quantitative quality information (RainGaugeQC), Atmos. Meas. Tech., 15, 5581–5597, https://doi.org/10.5194/amt-15-5581-2022, 2022.
- Ośródka, K., Szturc, J., Jurczyk, A., and Kurcz, A.: Adaptation of RainGaugeQC algorithms for quality control of rain gauge data from professional and non-professional measurement networks, Atmos. Meas. Tech., 18, 3229–3245, https://doi.org/10.5194/amt-18-3229-2025, 2025.
- Ouyang, L., Lu, H., Yang, K., Leung, L. R., Wang, Y., Zhao, L., Zhou, X., Lazhu, Chen, Y., Jiang, Y., and Yao, X.: Characterising uncertainties in ground "truth" of precipitation over complex terrain through high-resolution numerical modeling, Geophys. Res. Lett., 48, e2020GL091950, https://doi.org/10.1029/2020GL091950, 2021.
- Overeem, A., Leijnse, H., and Uijlenhoet, R.: Two and a half years of country-wide rainfall maps using radio links from commercial cellular telecommunication networks. Water Resour. Res., 52, 8039–8065, https://doi.org/10.1002/2016WR019412, 2016.
- Overeem, A., Leijnse, H., van der Schrier, G., van den Besselaar, E., Garcia-Marti, I., and de Vos, L.: Merging with crowdsourced rain gauge data improves pan-European radar precipitation estimates, Hydrol. Earth Syst. Sci., 28, 649–668, https://doi.org/10.5194/hess-28-649-2024, 2024.
- Pasierb, M., Bałdysz, Z., Szturc, J., Nykiel, G., Jurczyk, A., Ośródka, K., Figurski, M., Wojtczak, M., and Wojtkowski, C.: Application of commercial microwave links (CMLs) attenuation

- for quantitative estimation of precipitation, Meteorol. Appl., 31, e2218, https://doi.org/10.1002/met.2218, 2024.
- Peinó, E., Petracca, M., Polls, F., Udina, M., and Bech, J.: Intercomparison of H SAF and IMERG heavy rainfall retrievals over a Mediterranean coastal region, Atmos. Res., https://doi.org/10.2139/ssrn.5079222, in press, 2025.
- Perz, A., Wrzesiński, D., Budner, W. W., and Sobkowiak, L.: Flood-triggering rainfall and potential losses the copula-based approach on the example of the Upper Nysa Kłodzka River, Water, 15, 1958, https://doi.org/10.3390/w15101958, 2023.
- Putra, M., Rosid, M. S., and Handoko, D.: High-resolution rainfall estimation using ensemble learning techniques and multisensor data integration, Sensors, 24, 5030, https://doi.org/10.3390/s24155030, 2024.
- Rodwell, M. J., Haiden, T., and Richardson, D. S.: Developments in precipitation verification, ECMWF Newsletter, 128, 12–16, https://doi.org/10.21957/x49qpn1o, 2011.
- Schellart, A. N. A., Wang, L, and Onof, C.: High resolution rainfall measurement and analysis in a small urban catchment, in: 9th International Workshop on Precipitation in Urban Areas: Urban Challenges in Rainfall Analysis, UrbanRain 2012, ETH Zurich, 115–120, ISBN 978-390603121-7, 2017.
- Sideris, I. V., Gabella, M., Erdin, R., and Germann, U.: Real-time radar-rain-gauge merging using spatio-temporal co-kriging with external drift in the alpine terrain of Switzerland, Q. J. Roy. Meteorol. Soc., 140, 1097–1111, https://doi.org/10.1002/qj.2188, 2014
- Sinclair, S. and Pegram, G.: Combining radar and rain gauge rainfall estimates using conditional merging, Atmos. Sci. Lett., 6, 19–22, https://doi.org/10.1002/asl.85, 2005.
- Skamarock, W. C., Klemp, J. B., Dudhia, J., Gill, D. O., Liu, Z., Berner, J., Wang, W., Powers, J. G., Duda, M. G., Barker, D. M., and Huang, X.-Y.: A description of the Advanced Research WRF version 4, NCAR Tech. Note NCAR/TN-556+STR, NCAR, 145 pp., https://doi.org/10.5065/1dfh-6p97, 2019.
- Skok, G.: A new spatial distance metric for verification of precipitation, Appl. Sci., 12, 4048, https://doi.org/10.3390/app12084048, 2022
- Sokol, Z., Szturc, J., Orellana-Alvear, J., Popová, J., Jurczyk, A., and Célleri, R.: The role of weather radar in rainfall estimation and its application in meteorological and hydrological modelling A review, Remote Sens., 13, 351, https://doi.org/10.3390/rs13030351, 2021.
- Subba, S., Ma, Y.-M., Ma, W.-Q., and Han, C.-B.: Extreme precipitation detection ability of four high-resolution precipitation product datasets in hilly area: a case study in Nepal, Adv. Clim. Change Res., 15, 390–405, https://doi.org/10.1016/j.accre.2024.05.005, 2024.
- Sun, Q., Miao, C., Duan, Q., Ashouri, H., Sorooshian, S., and Hsu, K.-L.: A review of global precipitation data sets: Data sources, estimation, and intercomparisons, Rev. Geophys., 56, 79–107, https://doi.org/10.1002/2017RG000574, 2018.
- Szalińska, W., Otop, I., and Tokarczyk, T.: Precipitation extremes during flooding in the Odra River Basin in May–June 2010, Meteorol. Hydrol. Water Manage., 2, 13–21, https://doi.org/10.26491/mhwm/22918, 2014.
- Szturc, J., Ośródka, K., Jurczyk, A., Otop, I., Linkowska, J., Bochenek, B., and Pasierb, M.: Quality control and verification of precipitation observations, estimates, and forecasts, in: Precip-

- itation Science. Measurement, Remote Sensing, Microphysics and Modeling, edited by: Michaelides, S., Elsevier, 91–133, https://doi.org/10.1016/B978-0-12-822973-6.00002-0, 2022.
- Tanessong, R. S., Vondou, D. A., Djomou, Z. Y., and Igri, P. M.: WRF high resolution simulation of an extreme rainfall event over Douala (Cameroon): a case study, Model. Earth Syst. Environ., 3, 927–942, https://doi.org/10.1007/s40808-017-0343-7, 2017.
- Tapiador, F. J., Navarro, A., García-Ortega, E., Merino, A., Sánchez, J. L., Marcos, C., and Kummerow, C.: The contribution of rain gauges in the calibration of the IMERG product: Results from the first validation over Spain, J. Hydrometeorol., 21, 161–182, https://doi.org/10.1175/JHM-D-19-0116.1, 2020.
- Tarek, M., Brissette, F., and Arsenault, R.: Uncertainty of gridded precipitation and temperature reference datasets in climate change impact studies, Hydrol. Earth Syst. Sci., 25, 3331–3350, https://doi.org/10.5194/hess-25-3331-2021, 2021.
- Thompson, G., Rasmussen, R. M., and Manning, K.: Explicit forecasts of winter precipitation using an improve bulk microphysics scheme. Part I: Description and sensitivity analysis, Mon. Weather Rev., 132, 519–542, https://doi.org/10.1175/1520-0493(2004)132<0519:EFOWPU>2.0.CO;2, 2004.
- van der Valk, L. D., Coenders-Gerrits, M., Hut, R. W., Overeem, A., Walraven, B., and Uijlenhoet, R.: Measuring rainfall using microwave links: the influence of temporal sampling, Atmos. Meas. Tech., 17, 2811–2832, https://doi.org/10.5194/amt-17-2811-2024, 2024.
- Velásquez, N., Krajewski, W. F., and Seo, B.: Assessing the impact of radar-rainfall uncertainty on streamflow simulation, J. Hydrometeorol., 26, 169–184, https://doi.org/10.1175/JHM-D-24-0047.1, 2025.
- Wijayarathne, D., Coulibaly, P., Boodoo, S., and Sills, D.: Evaluation of radar-gauge merging techniques to be used in operational flood forecasting in urban watersheds, Water, 12, 1494, https://doi.org/10.3390/w12051494, 2020.
- WMO: No. 1257: Guide to Operational Weather Radar Best Practices, in: Volume VI: Weather Radar Data Processing, World Meteorological Organization, Geneva, 156 pp., https://library.wmo.int/records/item/69563-guide-to-operational-weather-radar-best-practices (last access: 17 July 2025), 2025.
- Yu, J., Li, X.-F., Lewis, E., Blenkinsop, S., and Fowler, H. J.: UKGr-sHP: a UK high-resolution gauge-radar-satellite merged hourly precipitation analysis dataset, Clim. Dynam., 54, 2919–2940, https://doi.org/10.1007/s00382-020-05144-2, 2020.
- Zhang, J., Howard, K., Langston, C., Kaney, B., Qi, Y., Tang, L., Grams, H., Wang, Y., Cocks, S., Martinaitis, S., Arthur, A., Cooper, K., Brogden, J., and Kitzmiller, D.: Multi-Radar Multi-Sensor (MRMS) quantitative precipitation estimation: Initial operating capabilities, B. Am. Meteorol. Soc., 97, 621–638, https://doi.org/10.1175/BAMS-D-14-00174.1, 2016.
- Zhang, Y., Wang, L., Li, Y., Wang, Y., Yao, F., and Chen, Y.: Impacts of reference precipitation on the assessment of global precipitation measurement precipitation products, Remote Sens., 17, 624, https://doi.org/10.3390/rs17040624, 2025.